MINERALIZATION PATTERN, MINERAL PHASES, AND SELECTED ELEMENTAL ANALYSIS OF THE DORSAL CARAPACE OF POSTECDYSIAL BLUE CRABS, *CALLINECTES SAPIDUS*

Samantha Johnson

A Thesis Submitted to the
University of North Carolina Wilmington in Partial Fulfillment
Of the Requirements for the Degree of
Master of Science

Department of Biology and Marine Biology

University of North Carolina Wilmington

2006

Approved by

Advisory Committee

_____Dr. Robert Roer_____ _____Dr. Thomas Shafer_____

_____Dr. Linda Potts_____ _____Dr. Richard Dillaman_____
Chair

Accepted by

_____Dr. Robert Roer_____
Dean, Graduate School

This thesis has been prepared in the style and format

consistent with the journal

Journal of Morphology

TABLE OF CONTENTS

ABSTRACT

The present investigation revealed the mineralization pattern, the mineral phases, and the selected elemental analysis of the dorsal carapace of the blue crab during postecdysis (1, 4, and 8 days) and intermolt (16 and 32 days) stages. Ten regions within the cuticle were examined using the scanning electron microscope (SEM) in secondary electron (SE), back-scattered electron (BSE), and x-ray microanalysis modes. X-ray microanalysis data were statistically analyzed using CATMOD (SAS). Amorphous mineral, presumably amorphous calcium carbonate (ACC) or amorphous calcium phosphate (ACP) was present in all regions of the cuticle and transformed to calcite or calcium phosphate over time in a spatial and temporal pattern for most regions. The middle and lower regions of the interprismatic septae were the only regions where the mineral did not transform with time. The statistical analyses of the quantitative data from x-ray microanalysis showed that the concentrations of selected elements relative to carbon and the P/Ca and Mg/Ca ratios changed within and among the regions of the cuticle over time. The results also suggested that there are three elementally distinct regions in the cuticle: the epicuticle and the distal exocuticle (EDE), the exocuticle, and the endocuticle. This study suggests that *Callinectes sapidus* uses ACC for its isotropic properties and as a precursor phase to a more stable, crystalline mineral. Amorphous mineral in combination with a crystalline phase may be used by blue crabs to create an exoskeleton with superior mechanical properties.

ACKNOWLEDGEMENTS

I would like to thank Dr. Richard Dillaman, my advisor, for giving me the opportunity to work in his lab, for his support, patience, and kindness. I also would like to express my gratitude to Mark Gay who taught me how to use the electron microscopes, how to process the tissue, how to solve computer problems, and who helped me continuously throughout this process. A special thanks to Dr. Thomas Shafer, Dr. Bob Roer, and Dr. Linda Potts, my committee members, who volunteered their time to support and guide me through this project. Thank you to Dr. Steve Emslie for being my mentor while I was an undergraduate, for taking me to the Southern Hemisphere Ornithology Conference in Brisbane, Australia (2000), and for encouraging me to attend graduate school.

To my family and friends who have given me unlimited support, words of encouragement, and unconditional love throughout this process – thank you from the bottom of my heart. I couldn't have done this without you! A big thanks to my fellow co-workers and friends at the NC Aquarium that always kept me smiling.

DEDICATION

I would like to dedicate this thesis to my mother, Jane Riddle Puckett and to my two grandmothers, Ella Mae Riddle and Bonnie Johnson, whose strength, wisdom, encouragement, and love mean so much to me - I will be forever grateful.

LIST OF TABLES

LIST OF FIGURES

INTRODUCTION

Biomineralization is a cell-mediated process in which organisms form minerals and is thought to have begun approximately 350 million years ago (Knoll, 2003). The term biomineral refers to composites of crystals and the associated organic matrix. Biominerals can be complex and have many distinguishing properties that include external morphology, crystallinity, isotropy, and varying trace element compositions (Weiner and Dove, 2003). At present, 64 different minerals have been identified from 55 phyla (Weiner and Dove, 2003). Fifty percent of the minerals that are formed by organisms contain calcium, while 25% are phosphates (Lowenstam and Weiner, 1989). Research on biomineralization began in the 1930's and has been focused on understanding the processes and control mechanisms that organisms use to form hard structures (Lowenstam and Weiner, 1989). Teeth, bones, shells, and exoskeletons of crustaceans are just a few of the hard structures that have been studied in the search for an understanding of the process of biomineralization (Roer and Dillaman, 1984; Lowenstam and Weiner, 1989).

The crustacean cuticle has four distinct layers starting with the outermost epicuticle, then the exocuticle, the endocuticle, and finally the membranous layer (Fig. 1). These layers are composed of an organic matrix that is approximately 70% chitin and 30% proteins (Welinder, 1974) and mineral that is mostly $CaCO_3$, (75-80%) with smaller amounts of $Ca_3(PO_4)_2$ (10-20%), $MgCO_3$ (5-15%) and other crystals (Dalingwater and Mutvei, 1990). The epicuticle has two layers: (1) a thin, impermeable external cover with spine projections protruding from the surface and (2) a thicker inner layer (Travis, 1963; Hegdahl et al., 1977b; Compère, 1995). The epicuticle is composed of lipoproteins and calcium salts, but lacks lamellae and chitin (Travis, 1965; Green and Neff, 1972; Welinder, 1975; Roer and Dillaman, 1984). The epicuticle borders

Fig. 1. a: A schematic representation (modified from Dalingwater and Mutvei, 1990) and SEM images of the four layers in the crustacean cuticle of *Callinectes sapidus*. The four layers shown are the epicuticle (Ep), exocuticle (Ex), endocuticle (En), and the membranous layer (ml). Within the cuticle, a pore canal (pc) extends from the hypodermis (hy) to the inner epicuticle. The exocuticle has interprismatic septae (IPS) that are polygonal imprints left by the epidermal cells after cuticle deposition. b: SEM images of fractured crab cuticle showing the morphology of the four layers. b1-2: Fractured cuticle showing the vertical fibers and homogeneous matrix of the epicuticle. b3: One-day cuticle showing the mineralized IPS (arrow) and the less mineralized prisms (arrowhead) in the exocuticle. b4: Secondary electron image showing the fine woven lamellae in the exocuticle that are embedded with mineral. b5: A fractured cuticle showing the thick, coarse lamellae of the endocuticle intertwined with fibers (arrow). b6: A high magnification image showing the fiber bundles of the endocuticle that form long rod-shaped elements. b7: A fracture showing the membranous layer as thin lamellae that are horizontal to the cuticle surface.

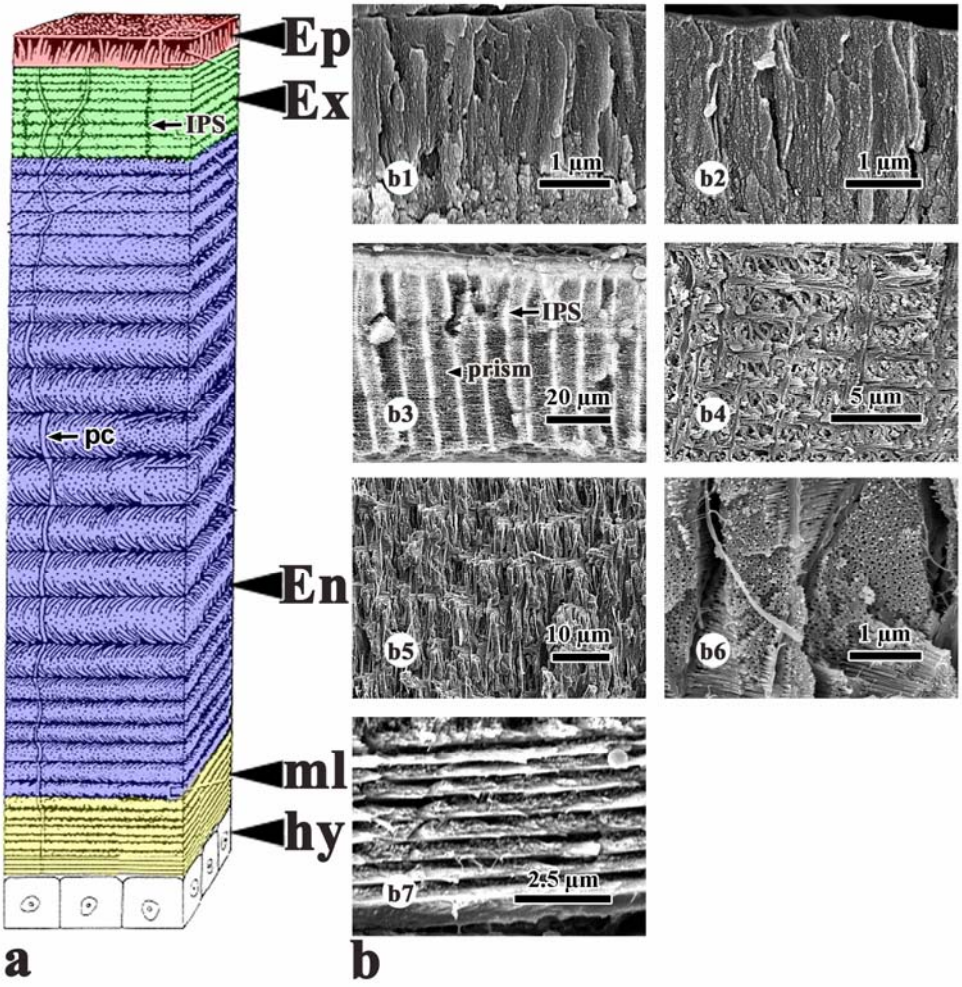
Ep
Ex
IPS
pc
En
ml
hy
a
b1
1 µm
b2
1 µm
IPS
prism
b3
20 µm
b4
5 µm
b5
10 µm
b6
1 µm
b7
2.5 µm
b

the distal portion of the exocuticle where there is a 5-15 μm thick prism-less zone that was called "zone externe" by Drach (1939) and referred to as the epicuticle/exocuticle border by Dillaman et al. (2005). It has been suggested that this zone or border differs in chemical composition from the other regions in the cuticle (Modla, 2006).

The exocuticle, a pigmented layer, represents approximately 25% of the cuticle and is composed of the interprismatic septae (IPS) and prisms that have a chitin-protein matrix with acid mucopolyssacharides and pore canals (Travis, 1965). The IPS are assumed to be polygonal imprints that are left in the exocuticle by the lateral margins of epidermal cells after cuticle deposition (Giraud-Guille, 1984). The matrix of the exocuticle and endocuticle are both highly organized and composed of lamellar sheets that stack and rotate through 360 degrees in a twisted helicoid or plywood-like arrangement that imparts strength to the cuticle (Bouligand, 1972; Green and Neff, 1972; Hadley, 1986). In the endocuticle, the chitin-protein matrix has a coarser structure with thicker lamellae, each layer averaging 35.1 μm thick, while the exocuticle has finer woven lamellae each with a height of only 9.4 μm (Raabe et al., 2005). The endocuticle comprises approximately 75% of the total cuticle thickness and is often referred to as the principal layer (Hegdahl et al., 1977c). Unlike the epicuticle and exocuticle, which are tanned, the endocuticle is untanned and hardened only by calcium salts (Drach, 1939; Roer and Dillaman, 1984).

The membranous layer is the innermost layer and is composed of unmineralized chitin and other organics. The membranous layer is characterized by thin lamellae that are parallel to the cuticle surface (Travis, 1965). The hypodermis is located under the membranous layer and is comprised of epithelial cells that are responsible for the formation of new cuticular layers after apolysis (Green and Neff, 1972; Roer and Dillaman, 1984). Numerous pore canals penetrate

through the cuticle to form a three dimensional system of cytoplasmic extensions that extend vertically from the hypodermis to the inner layer of the epicuticle (Compère and Goffinet, 1987). The pore canals function to actively transport ions for mineralization to the distal cuticular layers after ecdysis (Roer and Dillaman, 1984). The pore canals grow toward the hypodermis as new layers are formed, while degrading at their distal ends near the outermost portion of the cuticle. By intermolt, the pore canals have completely retracted from the cuticular layers and mineralization is thought to be complete (Compére and Goffinet, 1987b).

The exoskeleton is important in crustaceans because it provides protection, support, a site for muscle attachment for movement, and prevents water loss (Hadley, 1986). However, in order to grow crustaceans must shed their old exoskeleton. The frequency at which a crab molts is influenced by many factors (environment, size, developmental stage, reproductive maturity, and status of limb regeneration), but usually occurs once or twice a year in adults (Passano, 1960; Roer and Dillaman, 1984; Chang, 1995). The molt cycle is divided into five major stages based on the hardness of the exoskeleton (Drach, 1939). According to Drach, these five stages (A,B,C,D, and E) are: pre-ecdysis (D_0-D_4), ecdysis (E), postecdysis (A_1, A_2, B_1, B_2, C_1, C_2, C_3) and intermolt (C_4). The molt cycle is regulated by two major hormones (Drach, 1939; Roer and Dillaman, 1984). The hormone ecdysone stimulates molting while the molt-inhibiting levels during intermolt (Watson et al., 1998).

The molt cycle begins during pre-ecdysis when the hypodermis releases a molting fluid with digestive enzymes into the endocuticle and membranous layers. The organic and inorganic constituents are reabsorbed by the hypodermis (Roer, 1980). After degradation of these layers is complete, the hypodermis separates from the old cuticle (apolysis) and subsequently deposits a new epicuticle and exocuticle, the pre-exuvial layers (Drach, 1939, Travis, 1965). At ecdysis,

the entire cuticle becomes hydrated and causes an increase in hydrostatic pressure. As a result of the increased pressure, the posterior end of the old carapace breaks along the suture line and the crab pushes itself out of the old exoskeleton in a matter of minutes. After ecdysis, the crab increases in size by approximately 25-40% (Hill et al., 1989). The new exoskeleton remains soft and pliable, making it vulnerable to predation. Consequently, the crab forms a temporary hydrostatic skeleton that allows rapid and forceful movements for protection (Taylor and Kier, 2003). The soft crab begins calcifying the exoskeleton approximately three hours after ecdysis (Dillaman et al., 2005). In postecdysis, the epicuticle is hardened by tanning and calcification, which is a process that cross-links proteins with quinones (Travis, 1965; Giraud-Guille, 1984). The exocuticle is hardened by both tanning and calcification (Travis, 1955). The endocuticle is deposited while simultaneously being calcified (Drach, 1939; Travis and Friberg, 1963; Kramer et al., 1995). The last layer to be deposited is the membranous layer which does not mineralize. Its deposition marks the start of intermolt, the portion of the molt cycle where the adult crab spends most of its time (Passano, 1960). The cuticle at intermolt is thought to be completely deposited and fully mineralized (Drach, 1939; Green and Neff, 1972; Travis, 1955; Roer and Dillaman, 1993). The predictable, cyclic nature of molting in crustaceans makes it an excellent model for studying calcification (Lowenstam and Weiner, 1989).

Calcification is said to occur when calcium carbonate exceeds its solubility (Simkiss, 1975). However, calcification from supersaturated solutions is rarely seen as such a straightforward process governed only by solubility but has evolved in organisms to be a complex process with multiple control mechanisms (Addadi et al., 2006). Therefore, numerous investigations have been conducted to determine the "control mechanisms" of the mineralization process. Many studies propose that proteins in the matrix of the cuticle are involved in the

initiation and regulation of mineralization. It has been suggested that inhibitor proteins and polysaccharides regulate mineralization by preventing crystal nucleation (Wheeler et al., 1981). It has also been implied that the matrix can regulate the initiation of crystal growth, determine the crystal shape and phase, and stop crystal formation (Wheeler et al., 1988). Watson et al. (1998) had a more general conclusion than Wheeler, but again suggested that "the control of mineralization lies within the cuticle itself". Specifically, the matrix contains acidic proteins that can regulate crystal nucleation by binding to specific crystal faces and inhibiting growth or changing the direction of growth (Roer and Dillaman, 1993).

It has been shown using electrophoretic mobility and lectin affinity that EDTA-soluble proteins extracted from the cuticle of *Callinectes sapidus* changed dramatically between pre-ecdysis and postecdysial stages, with most of the changes occurring between one and three hours after ecdysis (Shafer et al., 1995). These dramatic changes are referred to as postecdysial cuticle alterations (PECA) and are thought to be important in the initiation of the calcification process, since these changes occur at the onset of mineralization. Coblentz et al. (1998) further investigated how these soluble proteins in the cuticle might regulate mineralization. They found that crystal-associated-proteins are present in the blue crab cuticle at all times and are attached to the organic matrix by acid-labile bonds. They also suggested that the crystal-associated-proteins serve as nucleation sites for calcium carbonate crystals, but the time at which nucleation begins is regulated by large macromolecules. These inhibitor proteins shield the nucleation sites from exposure to calcium and carbonate ions until one hour postecdysis when the macromolecule is removed or altered (Coblentz et al., 1998) by deglycoslation or proteolysis (Tweedie et al., 2004). The most recent study on the regulation of mineralization by proteins showed that a specific peptide (CAP-1) in the crayfish stabilized amorphous calcium carbonate, controlled the

deposition of calcium carbonate on the matrix and arranged the groups of acidic macromolecules by their interactions with chitin (Sugawara et al., 2006).

Over the molt cycle, the hypodermis actively transports calcium to and from the cuticular layers through ion channels using a Ca^{+2} -ATPase and a Na^{+}/Ca^{+2} antiporter (Roer, 1980). During pre-ecdysis, the calcium is reabsorbed from the old exoskeleton and actively transported across the hypodermis to the hemolymph. After ecdysis, the hypodermis transfers the calcium back from the hemolymph to the newly deposited cuticular layers via pore canals (Roer and Dillaman, 1984). In marine crabs, most of the calcium and carbonate ions used for mineralization are taken up by the gills from seawater (Greenaway, 1985). Bicarbonate ions (HCO_3^-) can also be derived from metabolic CO_2 by carbonic anahydrase, an enzyme found in the cuticle (Cameron, 1985; Roer and Dillaman, 1993). The initial site of calcification in the crab cuticle is the epicuticle and the IPS (Giraud-Guille, 1984; Compère et al., 1993). The IPS start mineralizing at 3 hours postecdysis at the distal and proximal boundaries of the exocuticle and fill in bi-directionally with calcium (Hequembourg, 2002). After the IPS are calcified, the prisms between the septa fill in with mineral uni-directionally from the epicuticle to the endocuticle (Dillaman et al., 2005). The initial mineral phase in the dorsal carapace of the blue crab has been suggested to be amorphous calcium carbonate (ACC) that changes to a crystalline form of calcium carbonate, presumably calcite (Hequembourg, 2002; Priester et al., 2005; Dillaman et al., 2005).

The calcium carbonate system is the most abundant and widespread form of mineralized tissue (Travis, 1963). Calcium carbonate can form at least six phases, three are anhydrous (calcite, aragonite, and vaterite) and three are hydrated forms (monohydrocalcite, hexahydrate, and amorphous calcium carbonate) (Clarkson et al., 1992). Decapod crustaceans have the ability

to form calcium carbonate as amorphous or crystalline mineral, or as a mixture of both (Vinogradov, 1953). Calcium carbonate has also been found to co-exist with amorphous calcium phosphate (ACP) (Addadi et al., 2003).

ACC has been found in a diverse group of organisms such as cystoliths in leaves of higher plants (*Fiscus retusa*) that act as pH stabilizers (Taylor et al., 1993), the exoskeleton of the blue crab *Callinectes sapidus* (Roer and Dillaman, 1984; Hequembourg, 2002), the spicules of the sponge *Clathrina* sp. (Aizenberg et al., 1996), the larval spicules of a the sea urchin *Paracentrotus lividus* (Beniash et al., 1997), calcium storage granules in the midgut of the crustacean *Orchestria cavimana* (Raz et al., 2002), the inner core of dogbone spicules of the ascidian *Pyura pachydermatina* (Aizenberg et al., 2002), the skeleton of the giant prawn *Macrobrachium rosendergii* (Soejoko and Tjia, 2003), sternal deposits of the woodlouse *Porcellio scaber* (Becker et al., 2003), and the exoskeleton of the crayfish *Procambarus clarkii* (Sugawara et al., 2006). ACC is used by organisms in three ways. First, it allows for a temporary storage site for ions that can easily be deposited and redissolved. For example, terrestrial crustaceans use storage sites regularly because they have limited resources of mineral from the environment and must replace calcium mostly through food and water. The terrestrial woodlouse *P. scaber* stores ACC in the anterior sternites so that the mineral can be rapidly mobilized after ecdysis to harden the new exoskeleton (Fabritius and Ziegler, 2003; Ziegler, 1994; Becker et al., 2005). Secondly, it is used as a structural element. ACC is isotropic, which allows the mineral to form complex shapes and be mechanically stronger, than crystals that can have weak faces, due to an equal distribution of stress (Levi-Kalisman et al., 2000). It has been suggested that *C. sapidus* uses amorphous mineral initially to form honeycomb shaped IPS in the exocuticle to create a strong, corrugated layer that can endure stress (Dillaman et al., 2005).

Third, the soluble ACC is often used as a precursor phase that precedes the precipitation of a more stable, crystalline form (Levi-Kalisman et al., 2000). The Ostwald-Lussac Law states "the phase with the highest solubility forms preferentially during a sequential precipitation" (Nancollas, 1982; Lowenstam and Weiner, 1989). For example, the larvae of the sea urchin *P. lividus* use ACC as a transient precursor phase prior to forming the calcitic spicules of the mature sea urchin (Beniash et al., 1997). Crabs and lobsters also use precursor phases of ACC to stiffen their exoskeletons quickly after ecdysis for survival against predation (Prenant, 1927; Addadi et al., 2003).

Amorphous biominerals have been far less studied than the crystalline minerals, partially because they are hard to detect (Addadi et al., 2003). Amorphous minerals are defined as having different degrees of short-range order, not the long range order of crystals. They form from highly supersaturated solutions that have additives such as proteins and ions (Raz et al., 2000; Weiner and Dove, 2003). In ACC, phosphorus and magnesium ions substitute into the crystal lattice and create a random network structure that is disordered and highly soluble (Simkiss, 1994; Levi-Kalisman et al., 2000; Raz et al., 2000; Mann, 2001). ACC has a solubility product log k_{sp} of -6.04 at 25ºC compared with -8.42 for calcite (Clarkson et al., 1992). Consequently, due to their lack of a repeated lattice pattern, amorphous minerals do not display an x-ray or electron diffraction pattern. In fact, the absence of a diffraction pattern has been used to distinguish between amorphous and crystalline forms (Levi-Kalisman et al., 2000; Aizenberg et al., 2002).

In a previous study on the pattern of calcium carbonate deposition in the dorsal carapace of pre-ecdysis (D_2-D_3) and early postecdysis (0-48 h) blue crabs, it was observed that mineral at 12 hours postecdysis in the IPS and at the epicuticle/exocuticle border was partially soluble

(Hequembourg, 2002). It was suggested that the initial mineral phase was ACC that transformed to calcite along a front that followed the original deposition and was controlled by the matrix within the IPS. This sequence of mineral precipitation is thought to be beneficial to the crab due to ACC's isotropic properties that makes the cuticle strong soon after ecdysis (Dillaman et al., 2005). Another recent study on *Callinectes sapidus*, showed that the suture region was more soluble than the adjacent calcified cuticle citing differences in Ca/P and Ca/Mg ratios that were correlated with solubility (Priester et al., 2005).

The main objective of this study was to further investigate the pattern of calcium carbonate deposition in the dorsal carapace of postecdysial (1, 4, and 8 days) and intermolt (16 and 32 days) blue crabs. Blue crabs, *Callinectes sapidus*, were chosen for calcification studies due to their high abundance and availability and most importantly, because they molt frequently, allowing researchers to examine isolated and predictable mineral changes in the cuticle. To complete this investigation on the mineralization pattern and element composition in the dorsal carapace of postecdysial blue crabs, the following null hypotheses were tested:

1. $H_{0:}$ Amorphous mineral is not present in the cuticle between 1-32 days postecdysis.
2. $H_{0:}$ Amorphous mineral in the cuticle does not transform to a less soluble mineral phase in a predictable spatial and temporal pattern during postecdysis.
3. $H_{0:}$ Relative concentrations (atomic %) of calcium, magnesium, phosphorus, and oxygen and the ratios of certain elements do not differ within regions of the cuticle over time.
4. H_0: Regions of the dorsal carapace cuticle do not differ in element composition over 32 days postecdysis.

5. $H_{0:}$ Intermolt cuticle treated with water does not differ in element composition from untreated cuticle.

MATERIALS AND METHODS

Specimen Collection

In May of 2004 and 2005, male and female blue crabs with carapace widths ranging from 13.0 to 15.5 cm were obtained from Endurance Seafood, Kill Devil Hills, North Carolina, a commercial crab shedding facility where pre-ecdysial crabs were held in open flow-through tanks (5.3ppt salinity, pH 7.5, $[Ca^{++}]$ = 86ppm). Crabs were continuously observed and within a few minutes of ecdysis were placed in individually marked cages. One day after ecdysis, crabs were sacrificed on-site and cuticle tissue processed. Crabs used for extended postecdysis intervals (4, 8, 16, and 32 days) were transported on ice or in aerated water from Endurance Seafood to the North Carolina Aquarium at Fort Fisher. At the aquarium, the postecdysial crabs were held in individually-marked cages in a closed, recirculating saltwater system (32ppt salinity, pH 8.3, and $[Ca^{++}]$ = 330ppm) and fed daily until sacrificed. Five crabs at each time interval were sacrificed for non-dispersive x-ray microanalysis and three for morphology and subsequent water treatment studies. In addition, a 13 day crab was examined for the presence of a membranous layer.

Tissue Preparation for Microscopy

At the designated times, the branchial cuticles were removed from the left and right sides of the dorsal carapace. One side of the branchial cuticle was immediately placed in a cryotube

and plunged into liquid nitrogen. The other side was fixed in 2.5% glutaraldehyde in 0.2M sodium cacodylate, pH 7.4, at ~870mOsm for light microscopy. Samples in liquid nitrogen were transferred to a –70°C freezer where they were stored until lyophilization. After lyophilization, for approximately 2 days using a LABCONCO 4.5 freeze dryer, samples were carefully fractured into smaller pieces.

Scanning Electron Microscopy

Epoxy-Embedded Samples

Lyophilized pieces of the branchial cuticle were placed directly into Spurr's standard epoxy resin (Spurr, 1969), polymerized, cut with a jeweler's saw, and progressively polished with 600 to 2000 grit sandpaper to produce a smooth surface. The polished surfaces diminished geometry differences among the cuticle samples that could affect the interaction with the electron beam and, thus, affect x-ray microanalysis. The cuticle within the resin block was oriented perpendicular to the block's surface so that the various layers of the cuticle were exposed. The epoxy blocks were mounted on aluminum stubs with colloidal graphite (Ted Pella, Redding, CA), polished side facing up, and coated with 6 nm of platinum/palladium (80:20) using a Cressington 208 HR Sputter Coater (Cressington Scientific, Inc. Cranberry Township, PA).

Each epoxy-embedded sample was examined and images recorded using the Philips XL30S FEG scanning electron microscope in secondary electron (SE) or back-scattered electron (BSE) mode. The SE mode was used for examining changes in morphology of the cuticle over time. The BSE mode revealed the distribution of mineral within the cuticle due to its higher atomic number compared to the atoms in the matrix. Secondary electron images were collected

at an accelerating voltage of 5 kV with spot size 3 and working distances of 5 or 7.5 mm, while BSE images were collected at 20 or 25 kV with spot size of 4 and working distances of 5 or 7.5 mm.

Fractured Samples

Fractured samples were used in addition to embedded samples to try to reveal the cuticle structure and crystal morphology at the different time intervals. Fractures from lyophilized samples were mounted (fracture side up) on aluminum stubs with colloidal graphite (Ted Pella, Redding, CA) and coated with 6 nm of platinum/palladium (80:20) using the Cressington 208 HR Sputter Coater (Cressington Scientific, Inc. Cranberry Township, PA). The morphology of the cuticle was examined with the Philips XL30S FEG scanning electron microscope in SE (5 kV, spot size 3) or BSE modes (20 or 25 kV, spot size 4) at working distances of 5 or 7.5 mm. High magnification SE images were collected using a through-the-lens detector with a working distance of 5 mm, spot size of 3, and an accelerating voltage of 5 kV. BSE images were also taken of a 13 day fractured sample to determine the presence of a membranous layer.

Water treatment was conducted on comparable fractured samples. The cuticles were first fractured (exposing all the regions of the cuticle to water) and then placed in a beaker with 200 milliliters of distilled water with a pH of 6.8-7.4 for 30 minutes. The samples were subsequently dehydrated using acetone in an ascending order of 50%, 70%, 90%, and 100% twice for fifteen minutes each. Dehydrated samples were then placed in hexamethyldisalizane (HMDS) for 30 minutes in a vent hood before being placed on Whatman's #1 filter paper in a Petri dish overnight to allow for evaporation (Bray et al., 1993). The specimens were recoated with 6 nm of platinum/palladium and re-examined using the SEM. Determination of the soluble and non-soluble mineral phases was achieved by comparing BSE images before and after water treatment.

Digital images were processed using Adobe Photoshop 7.0.

X-Ray Microanalysis

The EDAX Phoenix non-dispersive x-ray microanalysis system (EDAX version 3.32) was used to measure the relative concentrations of elements as atomic percents and determine their distribution in the lyophilized cuticles. The software provided a "Holographic Peak Deconvolution" function that established a best fit line along the peaks of the spectra to aid in identifying all elements present in the cuticle. The endogenous elements found in the cuticle were carbon, oxygen, sodium, magnesium, phosphorus, chlorine, potassium, and calcium. The exogenous elements included were chromium, platinum, and palladium resulting from the coating of the samples. Ten regions were chosen for analysis that provided the best representation of the various sites within the cuticle. The regions examined were: (1) the epicuticle and distal exocuticle (EDE), (2-10) the upper, middle, and lower regions of the IPS, prism, and the endocuticle as shown in figure 2. For each of the ten regions, five spectra were collected at different locations within a region moving laterally across the cuticle (Fig. 2). The x-ray microanalysis quantitative data (atomic percents) for calcium, magnesium, phosphorus, and oxygen relative to carbon were compared to determine if there were significant differences in element composition within and among the regions of the cuticle over 32 days postecdysis. The atomic percents were averaged for statistical analyses. Standard conditions for x-ray microanalysis were: 1. accelerating voltage 25kV, 2. magnification 4000x, 3. spot size 4, 4. working distance of 7.5 mm, and 5. dead time 20-40% with count rates of approximately 1000 per minute. Analyses of element concentrations were done on squares with surface areas of 25 μm^2 at the sites of interest for all regions except the IPS and prisms, which due to their small size, were analyzed using squares with surface areas of 6.25 μm^2 at the sites of interest. The

Fig. 2. A back-scattered electron image of a resin embedded eight-day cuticle featuring the ten regions that were examined in the dorso branchial cuticle during postecdysis. The regions examined were: (1) the epicuticle and distal exocuticle (EDE), (2-10) the upper, middle, and lower regions of the IPS, prism, and the endocuticle. For each of the ten regions, five spectra were collected at different locations within a region moving laterally across the cuticle. Analyses of element concentrations were done on five squares (represented by the red squares) per region with surface areas of 25 μm^2 at the sites of interest for all regions except the interprismatic septa and prisms, which were analyzed using squares with surface areas of 6.25 μm^2 at the sites of interest due to their small size.

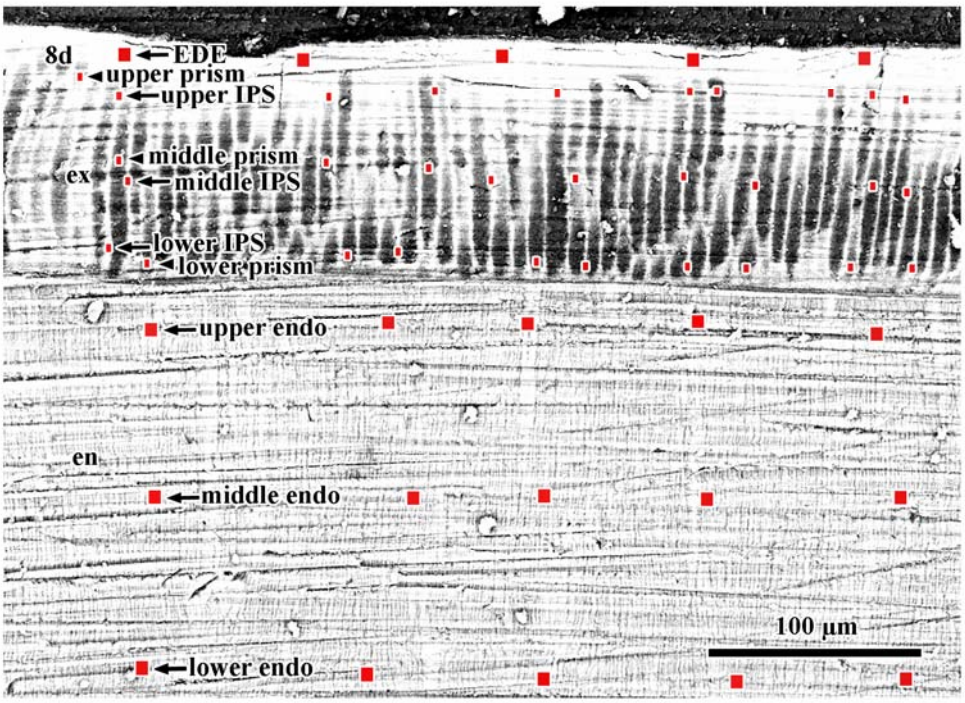
8d
EDE
upper prism
upper IPS
middle prism
ex
middle IPS
lower IPS
lower prism
upper endo
en
middle endo
100 μm
lower endo

spectra were collected for 200 live seconds. The escape peak function was used after the spectra were collected to remove background noise and peak interactions. Phosphorus to calcium and magnesium to calcium ratios were also graphed to visually compare differences among the regions of the cuticle over time.

X-ray microanalysis data were statistically analyzed using a baseline logit regression model (CATMOD Procedure, SAS9, SAS Institute, Cary, North Carolina), that assumed response data (elements) represented percentages among multinomial categories. The model included the factors region, time and their interaction. Carbon was used as the baseline in the model due to its high and relatively stable concentration. The significant differences, as tested by multiple contrasts that were constructed, were determined based on the Bonferroni adjustment. The Bonferroni adjustment is $\alpha = 0.05$ divided by the number of tests conducted and was used to decrease Type I errors. The significant difference value for elements changing within regions over time was $p \leq 0.0082$. The adjusted significant difference for the elemental differences between regions over time was $p < 0.00625$.

After images were collected and elemental analyses were completed on the dry epoxy-embedded samples, the top surfaces of the same samples were lightly sanded to re-expose the cuticle and then placed in distilled water for 30 minutes with a pH of 6.8-7.4 to determine if there was soluble mineral in the cuticle. The samples were subsequently dried in a vacuum chamber (4×10^{-3} Torr) for 30 minutes, recoated with 6 nm of platinum/palladium, and re-examined in the scanning electron microscope using both SE and BSE modes. Distributions of the mineral phases in the embedded samples were determined by comparing BSE images before and after water treatment. In addition to the previous work, x-ray microanalysis was used to re-examine the element composition of three 32 day samples after water treatment. Elemental analyses

(atomic %) of dry and wet 32 day samples were also compared using CATMOD.

Light Microscopy

The glutaraldehyde-fixed samples were decalcified in 10% EDTA with 0.1M Tris HCl, pH 7.4. The samples were then dehydrated using an ascending series of acetone, cleared in toluene, and embedded in paraffin. Once embedded, the samples were sectioned (9 μm thick) and then stained with hematoxylin and eosin following the protocol of Presnell and Schreibman (1997). One sample for each time period (1, 4, 8, 13, 16, and 32 days) was examined using the Olympus BH2 Light Microscope. Digital images were collected using a Spot RT 2 camera (Diagnostic Instruments, Inc.) and processed with Adobe Photoshop 7.0. The histological sections were used to determine the time at which intermolt occurred in crabs. Intermolt was detected by the presence of a membranous layer.

RESULTS

Scanning Electron Microscopy

Epoxy-embedded Samples

The BSE images of crab cuticle at one day postecdysis showed a bright BSE signal in the EDE, the vertical IPS in the exocuticle, and the endocuticle, suggesting that all of these regions were mineralized (Fig. 3a1). The prisms of the exocuticle had very little BSE signal, indicating that they contained little to no mineral. The BSE signal in the relatively thin endocuticle was homogeneous throughout, suggesting that mineral was evenly distributed. In contrast, the one-day embedded samples that were treated with water had a bright BSE signal in the EDE region, but the signal in the exocuticle was no brighter than that of the epoxy matrix (Fig. 3a2).

Fig. 3. BSE images of embedded crab cuticle before (a1, b1, c1) and after (a2-3, b2-3, c2-3) water treatment at one, four, and eight days postecdysis. a1: A one-day cuticle before water treatment showing a bright BSE signal for the EDE, the IPS (arrow), and the endocuticle (en). The prisms (arrowhead) have a low BSE signal indicating that there is little mineral content. a2-3: Cuticle after water treatment showing a loss of mineral in the IPS that appears as distinct voids (asterisks), the prisms, and the endocuticle. b1: A BSE image at four days showing a bright BSE signal for the EDE, distal portion of the exocuticle (ex), the regions of the IPS, and the endocuticle. b2: Four-day treated cuticle with mineral removed from the proximal external zone (asterisk), the upper region of the IPS, the regions of the prisms, and the endocuticle. c1: An eight day embedded cuticle displaying a similar distribution of mineral that was seen at four days. c2: Eight-day treated cuticle with mineral removed from the proximal external zone, the regions of the IPS, the middle and lower regions of the prisms, and the endocuticle. b3,c3: High magnification images showing mineral from the EDE extending down to the upper region of the IPS.

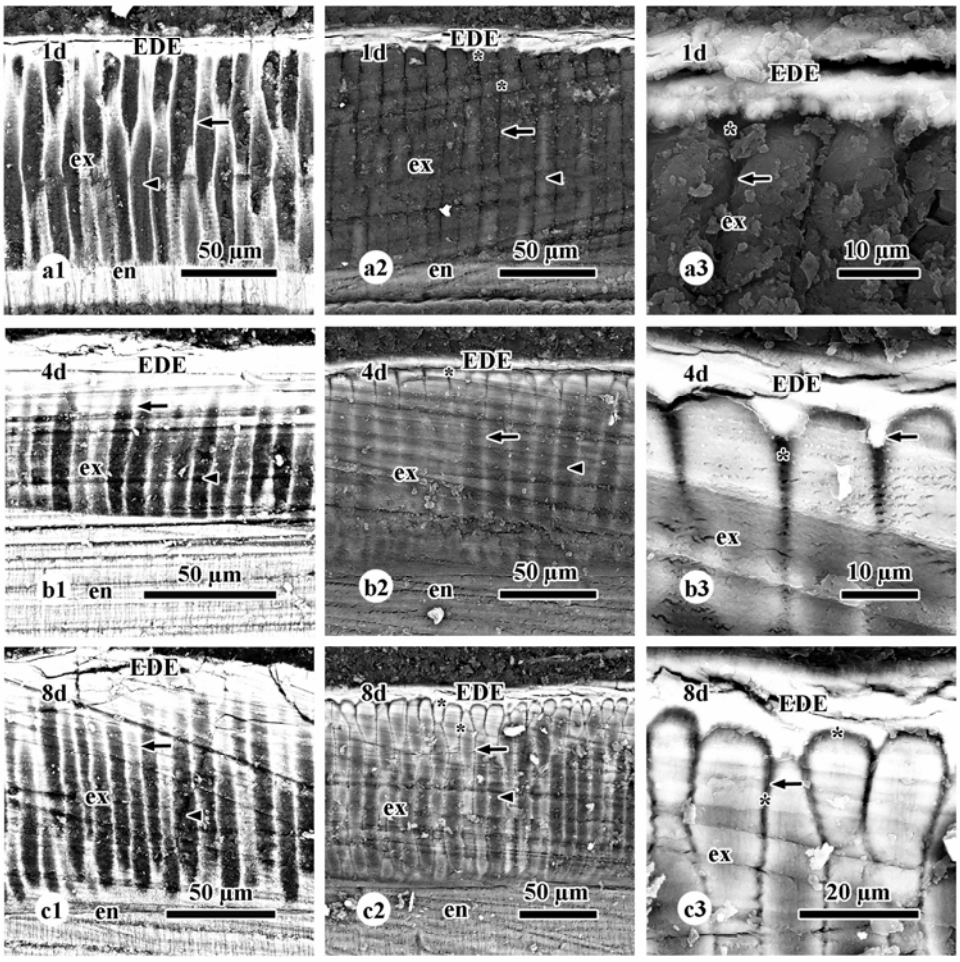
1d
EDE
ex
50 µm
a1
en
1d
EDE
ex
a2
en
50 µm
1d
EDE
ex
10 µm
a3
4d
EDE
ex
b1
en
50 µm
4d
EDE
ex
b2
en
50 µm
4d
EDE
ex
10 µm
b3
8d
EDE
ex
c1
en
50 µm
8d
EDE
ex
c2
en
50 µm
8d
EDE
ex
20 µm
c3

Particularly obvious were voids in the regions of the IPS suggesting the mineral there was highly soluble. The regions of the prism contained little mineral in the water treated samples at one day (cf. Fig. 3a1-2). The water treated endocuticle at one day had a low BSE signal and appeared darker than the untreated endocuticle (cf. Fig. 3a1-2). At high magnification, the area where the EDE met the upper region of the IPS and the upper region of the IPS itself were characterized by voids or deep crevices without mineral (Fig. 3a3).

The BSE images of four-day untreated cuticle had a bright BSE signal in the EDE, the upper region of the IPS, the upper region of the prisms, and the endocuticle that suggested these regions were mineralized (Fig. 3b1). The distal one-third of the exocuticle was heavily mineralized, making it hard to distinguish between the upper regions of the IPS and prisms. The middle and lower regions of the prisms had a BSE signal close to that of the epoxy matrix, indicating they contained little mineral. After water treatment, the four-day cuticles had mineral removed from the epicuticle/exocuticle border (also known as the proximal portion of the external zone), the upper region of the IPS, the prisms, and the endocuticle (Fig. 3b2). The proximal external zone and the upper region of the IPS had distinct voids. The distal 10% of the prisms had a brighter BSE signal than the middle and lower regions, but the mineral appeared less dense than untreated four-day cuticle (cf. Fig. 3b1-2). The next 20-50% of the prisms that included the lower portion of the upper prism, the middle region of the prism, and a small part of the lower region had a moderate BSE signal that was noticeably weaker than the untreated cuticle, but was not as dark as the epoxy matrix (Fig. 3b2). This suggested that at four days those regions of the prisms had a mixture of soluble and less soluble mineral. The lower region of the prisms had a low BSE signal (cf. Fig. 3b1-2). A higher magnification image of four-day

treated cuticle showed that the mineral in the EDE extended down into the upper region of the IPS (Fig. 3b3). Voids were seen below the crystallized
extensions in the upper region of the IPS.

The eight-day untreated embedded samples had cuticle morphology and mineral distribution similar to the four-day cuticle (cf. Fig. 3b1, c1). The EDE, IPS, and the endocuticle had a bright BSE signal (Fig. 3c1). The regions of the prisms varied in the intensity of their BSE signal with the upper region having the densest signal. The middle and lower regions of the prisms had a low BSE signal and appeared darker, suggesting that the mineral concentration was lower in these regions. Water treatment on the eight-day cuticles removed mineral in the proximal external zone, the regions of the IPS creating obvious voids, the middle and lower regions of the prisms, and the endocuticle (cf. Fig. 3c2-3). The distal 20% of the prisms had a bright and evenly distributed BSE signal that suggested again that the mineral was less soluble (cf. Fig. 3b2, c2-3). The middle and lower regions of the prisms and the endocuticle had a low BSE signal (cf. Fig. 3b2, c2). The mineral in the eight-day EDE was not removed by water treatment and appeared homogeneous. At high magnification, eight-day water treated cuticles had mineral extending from the EDE down to the upper region of the IPS (Fig. 3c3). Distinct voids outlined the tops of the prisms and extended down into the upper and middle regions of the IPS (cf. Fig. 3b3, c3).

At 16 days postecdysis, the untreated cuticles showed a bright BSE signal in the EDE, the distal portion of the exocuticle, the middle and lower regions of the IPS, and the endocuticle (Fig. 4a1). The middle and lower regions of the prisms had a lower BSE signal than the upper region. After water treatment, the BSE images of the cuticle at 16 days postecdysis had voids at the proximal edge of the external zone that outlined the upper regions of the prisms and in the

Fig. 4. BSE images of embedded crab cuticle before (a1, b1) and after (a2-3, b2-3) water treatment at 16, and 32 days postecdysis. a1: A view of the untreated 16-day cuticle showing a bright BSE signal for the EDE, the IPS (arrow), the upper and middle prisms, and the endocuticle (en). The lower regions of the prisms (arrowhead) have a low BSE signal and appear dark. a2: Treated 16-day cuticle showing a loss of mineral in the proximal edge of the external zone (asterisk) that outlined the top of the prisms, the middle and lower regions of the IPS, the prisms, and the endocuticle. a3, b3: High magnification images that show the mineral from the EDE extending further down into the upper region of the IPS. b1: A BSE image of 32-day untreated cuticle showing a bright BSE signal for the EDE, the regions of the IPS, the upper and middle regions of the prisms, and the endocuticle. b2: Treated 32-day cuticle showing a loss of mineral only in the lower portion of the upper region of the IPS and the middle and lower regions of the IPS (asterisks). c1-3: BSE images showing the thickness of the whole cuticle over time (1, 8, and 32 days).

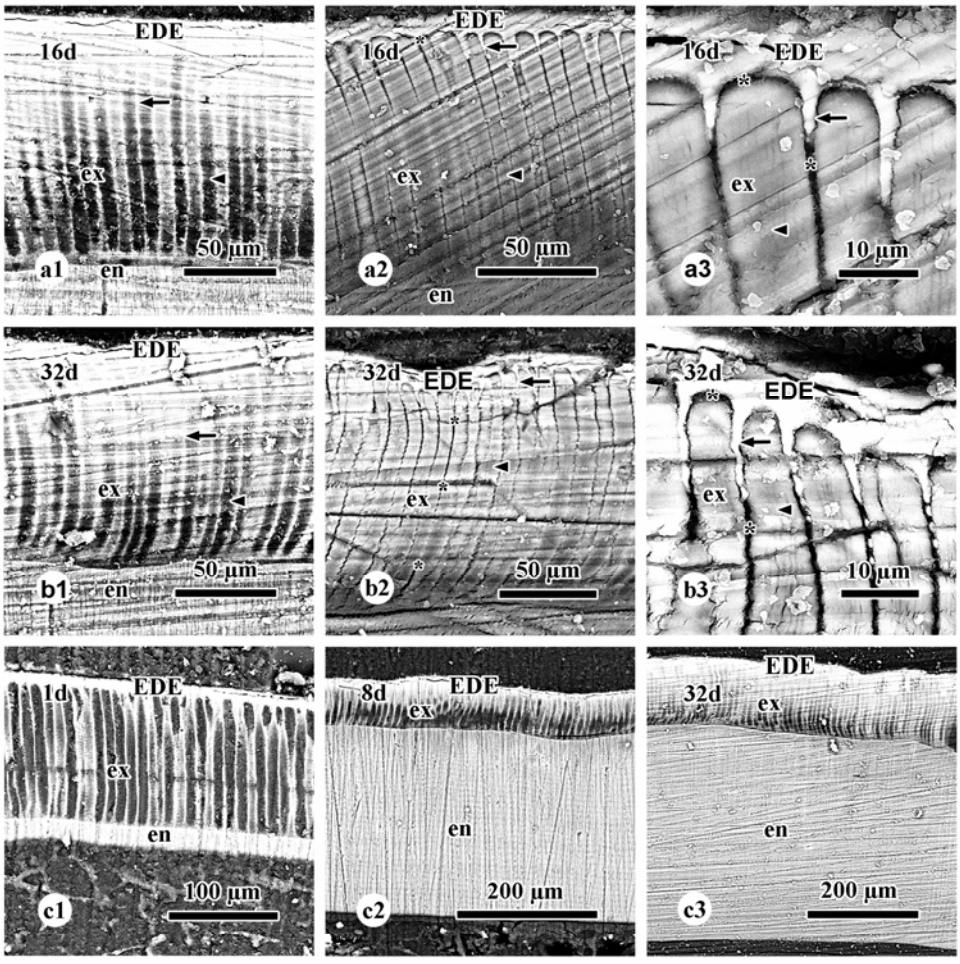
EDE
16d
ex
50 µm
a1
en
EDE
16d
ex
50 µm
a2
en
16d
EDE
ex
10 µm
a3
EDE
32d
ex
50 µm
b1
en
32d
EDE
ex
50 µm
b2
32d
EDE
ex
10 µm
b3
1d
EDE
ex
en
100 µm
c1
8d
EDE
ex
en
200 µm
c2
EDE
32d
ex
en
200 µm
c3

middle and lower regions of the IPS (cf. Fig. 4a2-3). The EDE had a bright BSE signal and appeared unchanged from the untreated 16-day cuticle (cf. Fig. 4a1-2). The upper and middle regions of the prisms had a reduced BSE signal when compared to the untreated sample, while the lower region of the prisms had little to no BSE signal. This suggested that the upper and middle regions of the prisms had a mixture of soluble and less soluble mineral phases even at 16 days postecdysis, while the lower region of the prisms still had little to no mineral. A high magnification image of a 16-day cuticle had mineral extending from the EDE to the upper region of the prisms and extending further down into the upper region of the IPS than shown at eight days postecdysis (cf. Figs. 3c3, 4a3). The middle region of the IPS appeared dark (Fig. 4a3).

The images of the untreated 32-day cuticles were similar to 16 days, except that the BSE signal for the middle region of the prisms was slightly brighter (cf. Fig. 4a1, b1). The regions of the IPS showed a brighter BSE signal than the regions of the prisms making them mostly distinguishable. The lower regions of the prisms had a low BSE signal compared to the distal 75% of the exocuticle. Consistent with cuticles examined from 1 to 16 days, the EDE and the endocuticle had a bright BSE signal. Water treatment of 32 day cuticles removed mineral in the lower portion of the upper region of the IPS, the middle region of the IPS, and the lower region of the IPS (Fig. 4b2). Most of the regions within the cuticle had a bright BSE signal that was unchanged from the untreated 32-day cuticle and this suggested that the mineral was less soluble at 32 days postecdysis (cf. Fig. 4b1-3). These regions were: the EDE, the proximal external zone, the upper region of the IPS, and the regions of the prisms. The upper, middle, and half of the lower region of the prisms had a bright BSE signal suggesting that the majority of the mineral in these regions was no longer very soluble, which differed from 16-day and earlier

water treated cuticles (cf. Fig. 4a2, 4b2). A high magnification image of a 32-day water treated cuticle showing the mineral from the EDE extending down the IPS margins (Fig. 4b3). Water treatment removed mineral in the middle region of the IPS and it appeared dark.

Cuticle thickness was measured over time (cf. Fig. 4c1-3). Thickness of the layers varied among samples. The epicuticle combined with the exocuticle (EDE) at one day postecdysis was approximately 10 μm thick, the remaining exocuticle was approximately 100 μm thick, while the endocuticle was approximately 20 μm thick (Fig. 4c1). The cuticle sample at eight days postecdysis had an exocuticle that was approximately 75 μm thick and an endocuticle approximately 275 μm thick (Fig. 4c2). The 32-day cuticle was approximately 4 times thicker than at day one (cf. Fig. 4c1-3). The combined epicuticle and exocuticle were approximately 100 μm thick, while the endocuticle had increased in thickness to approximately 390 μm (Fig. 4c3).

The endocuticles for all time periods were compared before and after water treatment. The same pattern was revealed in the endocuticle from 1 to 16 days, but changed between 16-32 days. Therefore, only the untreated and water treated embedded endocuticles for 16 and 32 days were compared at higher magnification (Fig. 5). The untreated cuticles for both time periods had a bright BSE signal and displayed vertical elements running down the cuticle (cf. Fig. 5a1, b1). However, after water treatment, the 16 and 32 day endocuticles differed in their mineral composition. The 16-day water treated cuticles had small, uniform 1 μm holes that were spaced approximately 1-4 μm apart forming horizontal rows throughout the endocuticle. The continuous rows of holes ran laterally across the cuticle and were separated by mineralized layers that were approximately 5-10 μm thick (Fig. 5a2). This suggested that the endocuticle was comprised of mostly insoluble mineral, but had small localized areas of soluble mineral from 1-

Fig. 5. Higher magnification images of the endocuticle before (a1, b1) and after (a2, b2) water treatment at 16 and 32 days postecdysis. a1, b1: BSE images of untreated endocuticles (en) at 16 and 32 days postecdysis have a bright BSE signal and vertical elements (arrow). a2: A view of water treated endocuticle at 16 days postecdysis displaying numerous small, uniform 1 μm holes (arrows) that form horizontal rows separated by mineralized layers (arrowheads). b2: A BSE image of a 32 day water treated endocuticle featuring etched crevices (arrow) in horizontal rows.

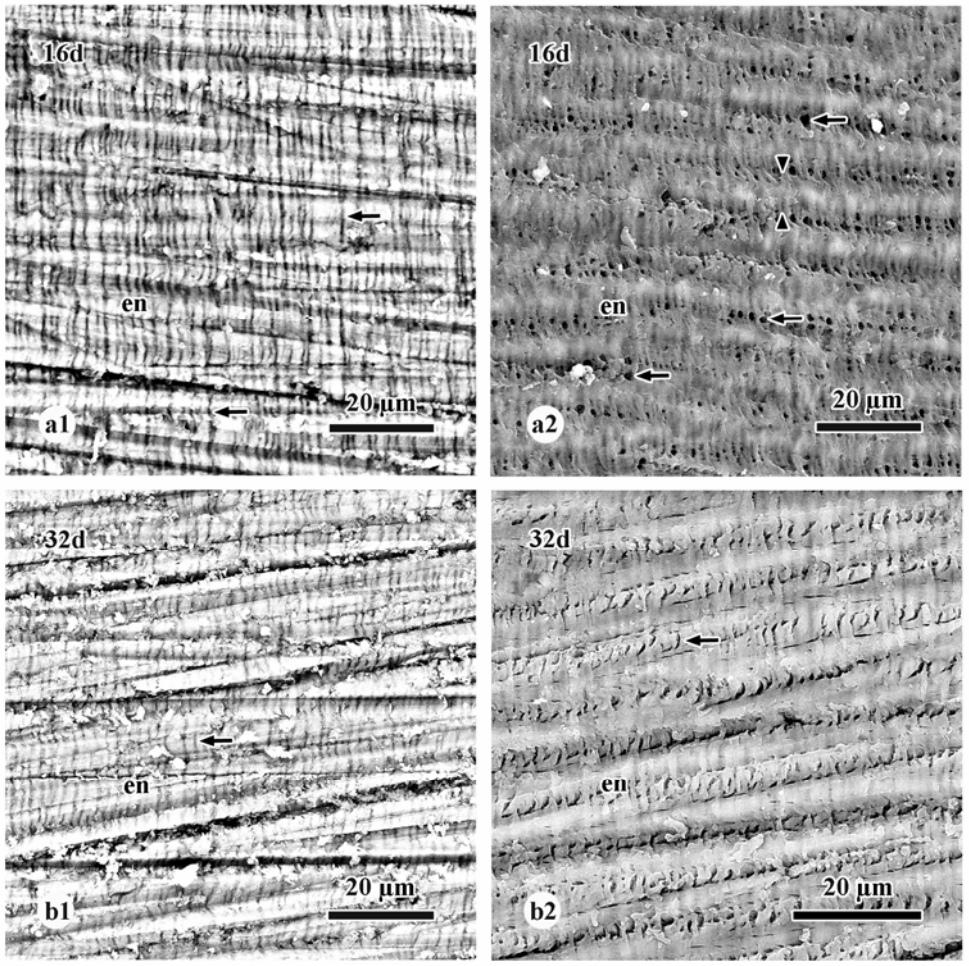
16d
en
20 µm
a1
16d
en
20 µm
a2
32d
en
20 µm
b1
32d
en
20 µm
b2

16 days postecdysis. In contrast, the 32-day water treated endocuticles did not contain holes, but had etched crevices in horizontal rows across the cuticle which differed from previous time periods, suggesting that the mineral in the holes was no longer soluble (Fig. 5b2).

Fractured samples

At one day postecdysis, the untreated, fractured cuticles had a bright BSE signal for the EDE and the IPS in the exocuticle (Fig. 6a1). The regions of the prisms at one day had a low BSE signal compared to the IPS regions suggesting that they contained less mineral than the IPS. The BSE images of one-day water treated cuticles had a bright BSE signal for the EDE, but a lower signal among the IPS and prisms regions compared to the untreated sample (Fig. 6a1-2). This revealed cuticular fibers.

The four-day untreated, fractured cuticles had a bright BSE signal for the EDE and the IPS, while the prisms had a low BSE signal (Fig. 6b1). After water treatment, the four day cuticles had a loss of mineral in the proximal external zone, the upper region of the IPS, and the middle and lower regions of the prisms (Fig. 6b2). The middle and lower regions of the prisms had a reduced, but moderate BSE signal when compared to the untreated sample, suggesting that soluble and less soluble mineral co-existed in these regions (cf. Fig. 6b1-2). The upper region of the prisms had a bright BSE signal and appeared unchanged from the untreated four-day sample (cf. Fig. 6b1-2). The EDE had a bright BSE signal and featured densely packed spherulites of mineral (Fig. 6b2).

At eight days, the untreated fractured samples had a morphology and mineral distribution similar to that of four day cuticle (cf. Fig. 6b1, c1). After water treatment, the four and eight day cuticles differed. At eight days the BSE signal in the middle region of the prisms was brighter than at four days (cf. Fig. 6b2, c2). This suggested that the mineral in the middle region of the

Fig. 6. BSE images of fractured cuticles before (a1, b1, c1) and after (a2, b2, c2) water treatment at one, four, and eight days postecdysis. a1: One-day untreated cuticle has a bright BSE signal for the EDE and the IPS (arrow) in the exocuticle (ex). The regions of the prisms (arrowhead) displaying a low BSE signal. a2: Cuticle after water treatment had a loss of mineral in the IPS and prisms regions. b1: Four-day untreated, fractured cuticle displaying a bright BSE signal for the EDE and the IPS (arrow), while the upper and middle regions of the prisms appeared darker (arrowhead). b2: A BSE image of water treated four-day cuticle showing that mineral was removed from the external zone (asterisk), the upper region of the IPS (asterisk), and the middle and lower regions of the prisms. c1: An eight-day untreated sample displaying a mineral distribution similar to that of four-day cuticle. c2: Eight-day cuticle after water treatment featuring voids in the proximal external zone and upper region of the IPS (asterisks).

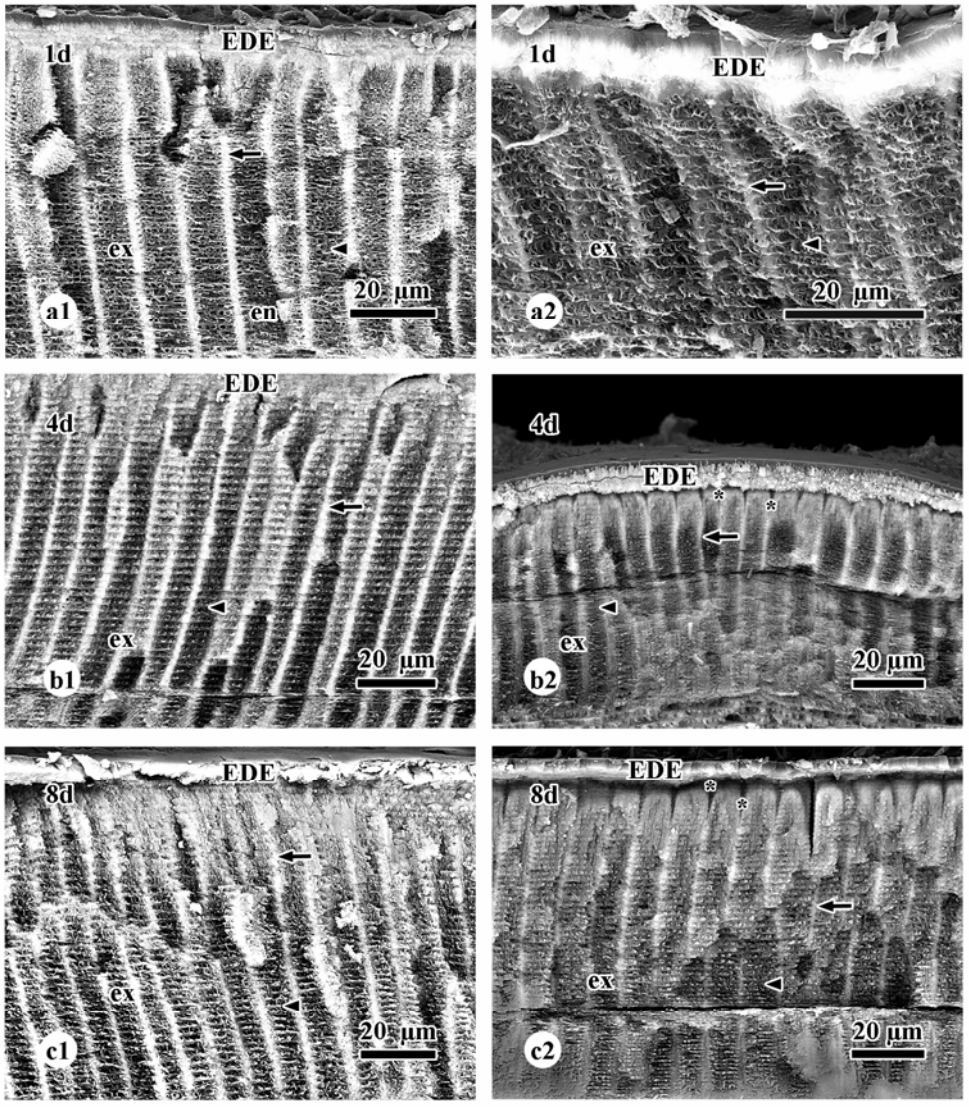
1d
EDE
ex
en
20 µm
a1
1d
EDE
ex
20 µm
a2
4d
EDE
ex
20 µm
b1
4d
EDE
ex
20 µm
b2
8d
EDE
ex
20 µm
c1
8d
EDE
ex
20 µm
c2

prisms was less soluble at eight days than at four days postecdysis. An extensive void or loss of mineral still appeared in the proximal external zone and upper region of the IPS after water treatment (Fig. 6c2). The IPS varied in the brightness of the BSE signal for most of the regions, but some of the IPS had a moderate or reduced signal.

Higher magnification images of the four-day water treated cuticle showed the morphology of the mineral in the EDE as spherulites that stacked on one another to make conglommerations of mineral that pointed toward the outer epicuticle from the distal exocuticle (Fig. 7). The aggregates of mineral did not extend all the way to the external surface of the cuticle, but quit approximately 1-2 μm from the impermeable layer to reveal a homogeneous matrix. A horizontal border that was approximately 7 μm thick was formed by the aggregates of mineral separating the external layer of the epicuticle from the upper regions of the IPS and prisms. The upper region of the IPS appeared as dark crevices with a fractured matrix. The area that outlined the upper region of the prism appeared etched and had a low BSE signal, suggesting there was a loss of mineral. Traces of pore canals were seen in the prisms as thin, vertical lines.

At 16 days, the untreated cuticles had a bright BSE signal for the majority of the cuticle (Fig. 8a1). In the distal half of the exocuticle, the BSE signal appeared bright and homogeneous. However, in the lower portion of the exocuticle the prisms appeared dark and could be distinguished from the IPS. The endocuticle was heavily mineralized. Water treatment of 16-day fractured cuticles removed mineral in the upper region of the IPS (Fig. 8a2). The distal portion of the EDE had a bright BSE signal and immediately below was a unique second and separate mineral layer that had not been seen in previous time periods (Fig. 8a2). The upper and middle regions of the prisms appeared unchanged when compared to the untreated fractured cuticle, suggesting that the mineral was not soluble (cf. Fig. 8a1-2).

Fig. 7. A higher magnification image of a four-day water-treated cuticle featuring the crystal morphology of the mineral in the EDE. The mineral appears as aggregates of spherulites that point toward the outer epicuticle from the distal exocuticle. The aggregates of mineral quit approximately 1-2 μm from the cuticle surface and reveal a homogeneous matrix (double-headed arrow). The upper region of the IPS (arrow) is dark with a fractured matrix. The area that outlines the upper region of the prism (asterisk) is etched and has a low BSE signal. Traces of pore canals in the prisms (arrowheads).

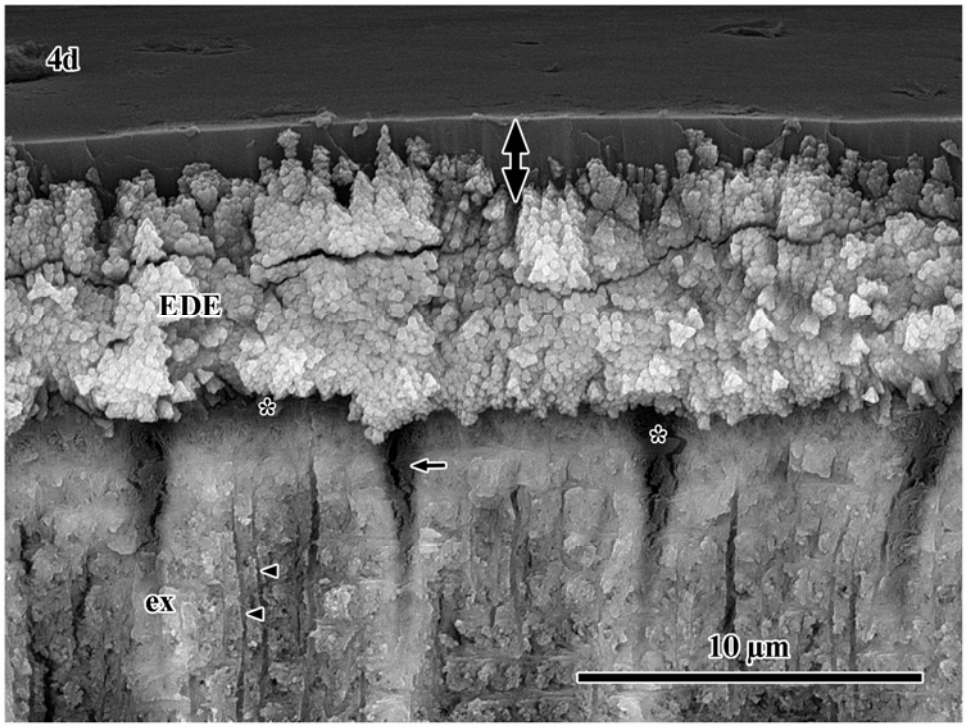
4d
EDE
ex
10 µm

Fig. 8. BSE images of fractured cuticle before (a1, b1) and after (a2, b2) water treatment at 16 and 32 days postecdysis. a1: Fractured 16-day cuticle before water-treatment showing a bright BSE signal for the EDE, the distal half of the exocuticle (ex), the middle and lower regions of the IPS (arrow), and the endocuticle. The lower region of the prisms have a low BSE signal (arrowhead). a2: Water treated 16-day cuticle had a loss of mineral in the upper region of the IPS (asterisk, arrow). A unique second and separate mineral layer was shown at 16 days (double-headed arrow). The upper and middle regions of the prisms at 16 days appeared unchanged from the untreated fractured cuticle. b1: A view of an untreated 32-day cuticle showing a bright BSE signal for the EDE and the distal three-fourths of the exocuticle, while the lower region of the prisms has a low BSE signal. b2: Treated 32-day cuticle showing the mineral in the EDE as one continuous layer that extended to the upper region of the IPS and prisms and a loss of mineral in the upper region of the IPS just below the mineral extensions (asterisk).

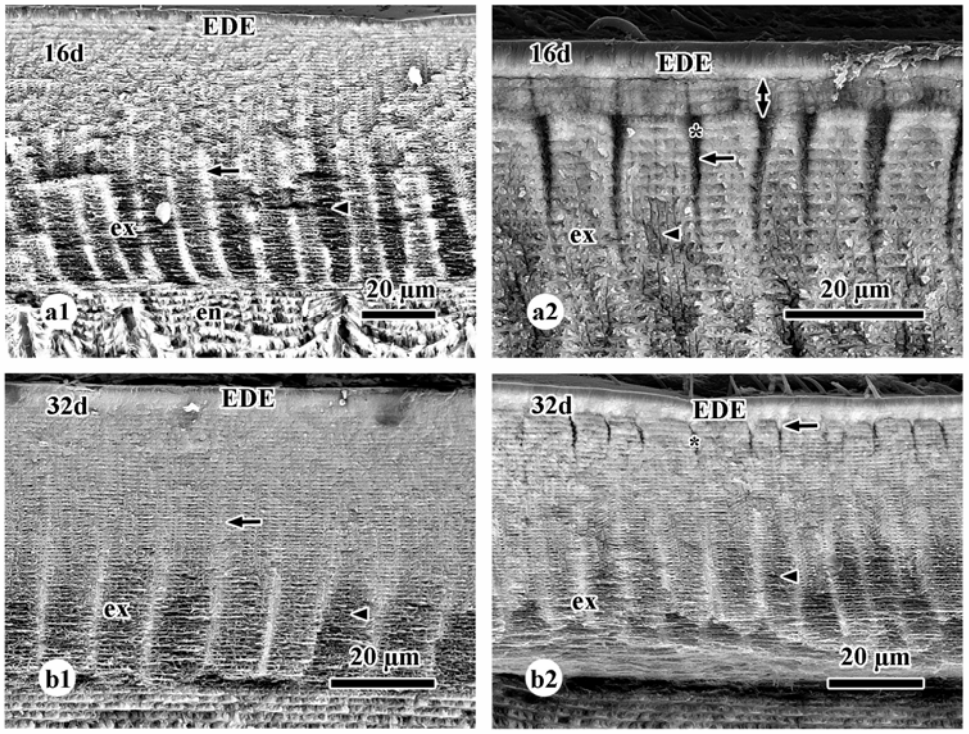
16d
EDE
ex
en
20 µm
a1
16d
EDE
ex
20 µm
a2
32d
EDE
ex
20 µm
b1
32d
EDE
ex
20 µm
b2

The BSE images of the untreated 32-day cuticles had a bright BSE signal for the EDE and the distal three-fourths of the exocuticle (Fig. 8b1). The lower region of the prisms had a lower BSE signal than the rest of the cuticle. This suggested that almost the entire cuticle was unmineralized at 32 days postecdysis, the exception being the lower region of the prisms. After water treatment, the 32 day fractured cuticles had an EDE that appeared to be one continuous layer of mineral that extended to the upper region of the prisms and filled in the upper region of the IPS (Figs. 8b2). A loss of mineral occurred only in the upper region of the IPS just below the mineral extensions. The middle and lower regions of the IPS appeared unchanged compared to the untreated cuticle (cf. Fig. 8b1-2). The upper and middle regions of the prisms had a bright BSE signal that was similar to the untreated sample, suggesting the mineral was not soluble at 32 days postecdysis (cf. Fig. 8b1-2). The lower regions of the prisms had a low BSE signal, similar to the untreated cuticle.

X-Ray Microanalysis

Since x-ray microanalysis was not based on equal sample volumes, values for elements were expressed as atomic percents. X-ray microanalysis showed that eight of the ten regions examined in the dorsal carapace increased in their mean relative concentrations of calcium, phosphorus, oxygen, and magnesium, while they decreased in carbon content over 32 days postecdysis (Tables 1a-d). The two regions that did not follow this trend were the middle and lower regions of the endocuticle, where phosphorus as well as carbon decreased relative to the other elements over time (Table 1d).

To statistically compare the relative percentages of the elements within and among regions at different times, the ratios of each element to carbon were used (Fig. 9). The EDE and upper region of the IPS had the highest ratios for all four graphs, whereas the regions of the

Table 1a. Mean relative concentrations (± standard errors) for selected elements in the epicuticle and distal exocuticle at 1-32 days postecdysis.

		Days postecdysis Atomic % (± S.E.)					Change
Region	Elements	1	4	8	16	32	32d-1d
EDE	Ca	13.57	14.28	13.06	15.74	16.43	+2.86
		(1.54)	(1.58)	(1.52)	(1.64)	(1.67)	
	P	0.36	1.62	1.47	1.47	1.86	+1.50
		(0.27)	(0.57)	(0.54)	(0.54)	(0.61)	
	O	35.20	43.12	44.20	43.74	43.48	+8.28
		(2.15)	(2.23)	(2.24)	(2.24)	(2.23)	
	Mg	1.08	1.71	1.90	1.97	2.03	+0.95
		(0.47)	(0.58)	(0.62)	(0.63)	(0.64)	
	C	49.78	39.27	39.37	37.08	36.20	-13.58
		(2.26)	(2.20)	(2.20)	(2.18)	(2.17)	

Table 1b. Mean relative concentrations (± standard errors) for selected elements in the upper, middle, and lower regions of the IPS 1-32 days postecdysis.

		Days postecdysis Atomic % (±S.E.)					Change
Regions	Elements	1	4	8	16	32	32d-1d
upper IPS	Ca	5.19	6.69	8.83	13.41	11.78	+6.59
		(1.00)	(1.13)	(1.28)	(1.54)	(1.46)	
	P	0.43	1.63	2.32	3.00	2.61	+2.18
		(0.29)	(0.57)	(0.68)	(0.77)	(0.72)	
	O	18.58	25.22	30.48	35.02	30.70	+12.12
		(1.75)	(1.96)	(2.08)	(2.15)	(2.08)	
	Mg	0.49	1.21	1.72	1.89	1.68	+1.19
		(0.32)	(0.49)	(0.59)	(0.61)	(0.58)	
	C	75.31	65.24	56.65	46.68	53.23	-22.08
		(1.94)	(2.15)	(2.24)	(2.25)	(2.25)	
middleIPS	Ca	4.51	4.55	5.78	8.36	8.21	+3.70
		(0.94)	(0.94)	(1.05)	(1.25)	(1.24)	
	P	0.29	0.98	1.59	1.91	1.85	+1.56
		(0.24)	(0.44)	(0.56)	(0.62)	(0.61)	
	O	18.11	18.84	22.71	26.17	23.53	+5.42
		(1.74)	(1.76)	(1.89)	(1.98)	(1.91)	
	Mg	0.40	0.76	1.18	1.26	1.25	+0.85
		(0.29)	(0.39)	(0.49)	(0.50)	(0.50)	
	C	76.69	74.87	68.75	62.30	65.16	-11.53
		(1.91)	(1.95)	(2.09)	(2.18)	(2.15)	
lower IPS	Ca	4.03	5.00	5.92	5.92	6.92	+2.89
		(0.89)	(0.98)	(1.06)	(1.06)	(1.14)	
	P	0.24	0.79	1.03	0.72	1.02	+0.78
		(0.22)	(0.40)	(0.46)	(0.38)	(0.45)	
	O	16.21	19.66	23.00	21.06	20.71	+4.50
		(1.67)	(1.79)	(1.90)	(1.84)	(1.83)	
	Mg	0.35	0.65	0.94	0.76	0.92	+0.57
		(0.27)	(0.36)	(0.43)	(0.39)	(0.43)	
	C	79.18	73.88	69.11	71.54	70.43	-8.75
		(1.83)	(1.98)	(2.08)	(2.03)	(2.06)	

Table 1c. Mean relative concentrations (± standard errors) for selected elements in the upper, middle, and lower regions of the prism 1-32 days postecdysis.

Regions	Elements	Days postecdysis Atomic % (±S.E.) 1	4	8	16	32	Change 32d-1d
upper prism	Ca	3.87	5.30	6.39	12.86	9.72	+5.85
		(0.87)	(1.01)	(1.10)	(1.51)	(1.49)	
	P	0.37	1.23	1.75	2.96	2.14	+1.77
		(0.27)	(0.50)	(0.59)	(0.76)	(0.73)	
	O	10.76	17.05	21.41	30.49	22.89	+12.13
		(1.40)	(1.70)	(1.85)	(2.08)	(2.12)	
	Mg	0.29	0.71	1.06	1.50	1.08	+0.79
		(0.24)	(0.38)	(0.46)	(0.55)	(0.52)	
	C	84.71	75.72	69.38	52.18	64.17	-20.54
		(1.62)	(1.93)	(2.08)	(2.25)	(2.42)	
middle prism	Ca	3.15	3.05	4.06	7.15	6.48	+3.33
		(0.79)	(0.77)	(0.89)	(1.16)	(1.11)	
	P	0.22	0.69	1.11	1.76	1.51	+1.29
		(0.21)	(0.37)	(0.47)	(0.59)	(0.55)	
	O	10.74	11.52	13.48	19.36	17.83	+7.09
		(1.40)	(1.44)	(1.54)	(1.78)	(1.72)	
	Mg	0.22	0.36	0.59	0.90	0.81	+0.59
		(0.21)	(0.27)	(0.35)	(0.43)	(0.40)	
	C	85.67	84.39	80.76	70.84	73.38	-12.29
		(1.58)	(1.64)	(1.78)	(2.05)	(1.99)	
lower prism	Ca	2.77	4.20	4.56	4.57	5.28	+2.51
		(0.74)	(0.90)	(0.94)	(0.94)	(1.01)	
	P	0.20	0.71	0.76	0.72	0.86	+0.66
		(0.20)	(0.38)	(0.39)	(0.38)	(0.42)	
	O	10.03	11.99	13.97	12.32	13.35	+3.32
		(1.36)	(1.46)	(1.56)	(1.48)	(1.53)	
	Mg	0.17	0.38	0.53	0.42	0.50	+0.33
		(0.19)	(0.28)	(0.33)	(0.29)	(0.32)	
	C	86.84	82.73	80.18	81.97	80.01	-6.83
		(1.53)	(1.70)	(1.80)	(1.73)	(1.80)	

Table 1d. Mean relative concentrations (± standard errors) for selected elements in the upper, middle, and lower regions of the endocuticle 1-32 days postecdysis.

Regions	Elements	Days postecdysis Atomic % (±S.E.) 1	4	8	16	32	Change 32d-1d
upper endo	Ca	9.50	9.51	9.65	10.74	11.01	+1.51
		(1.33)	(1.32)	(1.33)	(1.40)	(1.41)	
	P	0.84	0.85	1.05	1.13	1.21	+0.37
		(0.41)	(0.41)	(0.46)	(0.48)	(0.49)	
	O	28.56	31.97	31.80	31.37	31.75	+3.19
		(2.04)	(2.10)	(2.10)	(2.09)	(2.10)	
	Mg	0.69	0.91	1.05	1.09	1.12	+0.43
		(0.37)	(0.43)	(0.46)	(0.47)	(0.47)	
	C	60.42	56.76	56.45	55.66	54.90	-5.52
		(2.21)	(2.23)	(2.23)	(2.24)	(2.24)	
middle endo	Ca	10.38	11.03	9.97	11.77	12.82	+2.44
		(1.54)	(1.41)	(1.35)	(1.45)	(1.51)	
	P	1.02	0.78	0.90	0.74	0.65	-0.37
		(0.51)	(0.40)	(0.43)	(0.39)	(0.36)	
	O	29.78	35.65	34.77	33.31	34.65	+4.87
		(2.31)	(2.16)	(2.15)	(2.13)	(2.14)	
	Mg	0.74	0.93	0.99	1.05	1.07	+0.33
		(0.43)	(0.43)	(0.45)	(0.46)	(0.46)	
	C	58.07	51.61	53.37	53.13	50.82	-7.25
		(2.50)	(2.25)	(2.25)	(2.25)	(2.25)	
lower endo	Ca	8.50	10.46	10.19	10.68	11.66	+3.16
		(1.26)	(1.38)	(1.37)	(1.39)	(1.45)	
	P	0.84	0.41	0.31	0.08	0.46	-0.38
		(0.41)	(0.29)	(0.25)	(0.12)	(0.31)	
	O	27.55	34.09	32.09	31.57	31.90	+4.35
		(2.02)	(2.14)	(2.11)	(2.10)	(2.10)	
	Mg	0.67	1.03	0.95	0.92	0.92	+0.25
		(0.37)	(0.46)	(0.44)	(0.43)	(0.43)	
	C	62.44	54.02	56.47	56.75	55.06	-7.38
		(2.19)	(2.25)	(2.24)	(2.24)	(2.24)	

Fig. 9. Ratios of (a) phosphorus to carbon (b) magnesium to carbon (c) calcium to carbon and (d) oxygen to carbon for the ten regions examined over 32 days postecdysis.

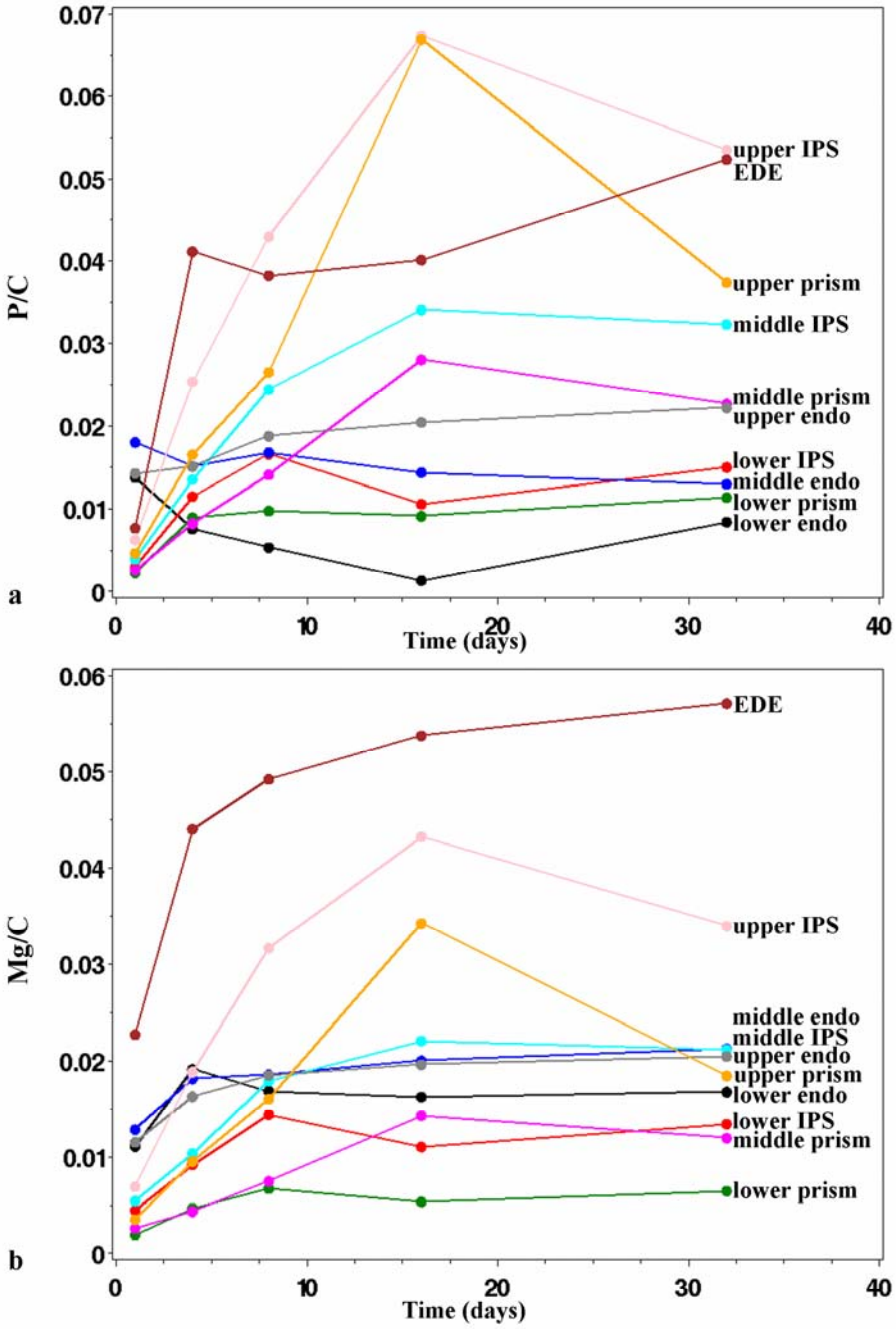
a
P/C
0.07
0.06
0.05
0.04
0.03
0.02
0.01
0
0
10
20
30
40
Time (days)
upper IPS
EDE
upper prism
middle IPS
middle prism
upper endo
lower IPS
middle endo
lower prism
lower endo
b
Mg/C
0.06
0.05
0.04
0.03
0.02
0.01
0
0
10
20
30
40
Time (days)
EDE
upper IPS
middle endo
middle IPS
upper endo
upper prism
lower endo
lower IPS
middle prism
lower prism

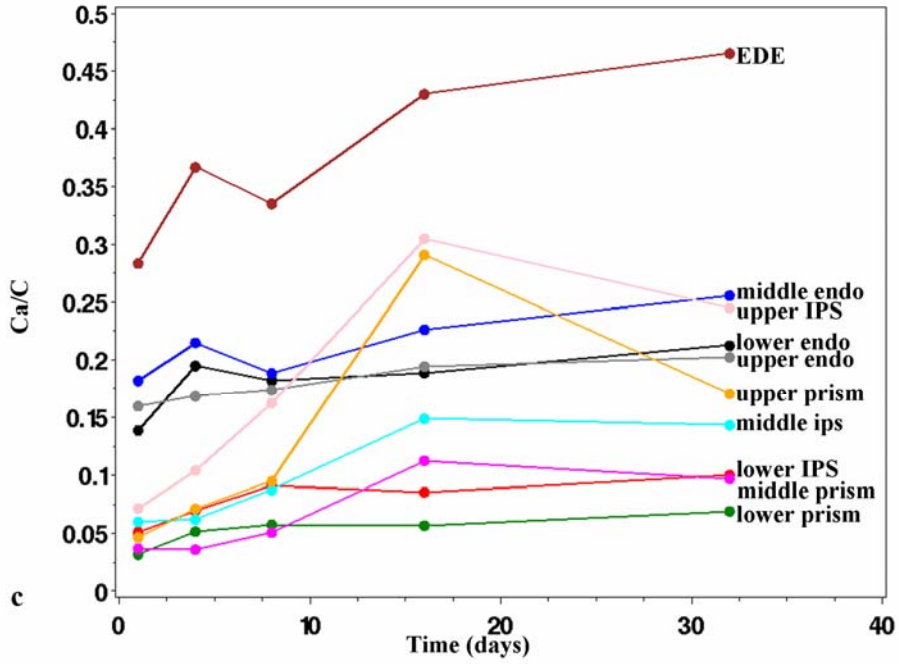
Ca/C
Time (days)
EDE
middle endo
upper IPS
lower endo
upper endo
upper prism
middle ips
lower IPS
middle prism
lower prism

c

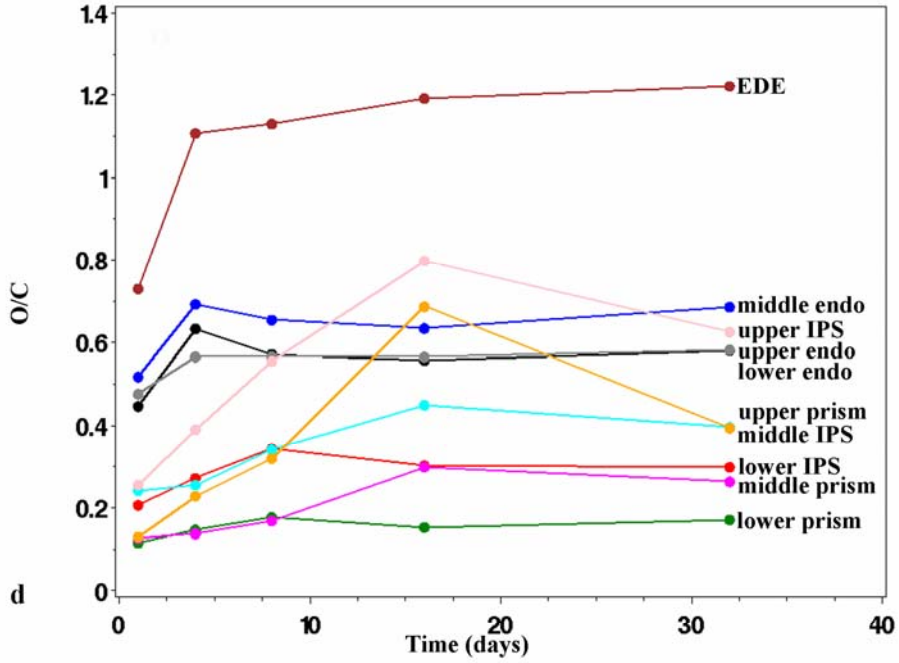
O/C
Time (days)
EDE
middle endo
upper IPS
upper endo
lower endo
upper prism
middle IPS
lower IPS
middle prism
lower prism

d

Table 2. Significant changes in concentrations (atomic %) relative to carbon for selected elements within the regions of the cuticle over 32 days postecdysis. The significant difference was $p \leq 0.0082$, highly significant $p \leq 0.0001$ denoted by *, and no significant difference (N.D.). The arrows indicate the direction of change in element concentration over time.

		Days postecdysis					
Regions/Elements		1-4	4-8	1-8	8-16	16-32	1-32
EDE	Ca		↓			↑	N.D.
	P						N.D.
	O						N.D.
upper IPS	Ca			↑*	↑	↓*	N.D.
	P					↓	↑
	O		↑	↑*	↑	↓*	↑*
middle IPS	Ca						N.D.
	P					↓	N.D.
	O	↑					N.D.
lower IPS	Ca				↓		N.D.
	P						N.D.
	O				↓*	↓*	N.D.
upper prism	Ca				↑*	↓*	↑
	P				↑	↓*	N.D.
	O	↑		↑*	↑*	↓*	↑*
middle prism	Ca				↑	↓*	N.D.
	P					↓	N.D.
	O				↑*	↓*	N.D.
lower prism	Ca				↓		N.D.
	P						N.D.
	O				↓	↑	N.D.
upper endo	Ca			↑		↑*	N.D.
	P			↑			N.D.
	O			↑*		↑*	↑
middle endo	Ca		↓	↑		↑*	N.D.
	P	↓		↓*		↓	N.D.
	O		↓	↑	↓	↑*	N.D.
lower endo	Ca				↑	↑*	N.D.
	P	↓*		↓*		↑	↓*
	O		↓*	↑	↓	↑*	N.D.

regions of the endocuticle had the lower ratios for P/C and Mg/C, but had the higher ratios for Ca/C and O/C (Fig. 9). Most changes in element concentration relative to carbon were not significant within the regions of from 1-32 days postecdysis (Table 2). The four regions that had significant changes in concentrations for the selected elements from 1-32 days were: the upper region of the IPS, the upper region of the prism, and the upper and lower regions of the endocuticle (Table 2). Oxygen concentration relative to carbon significantly increased over 32 days postecdysis within the upper region of the IPS, the upper region of the prism, and the upper region of the endocuticle. Phosphorus concentration relative to carbon significantly increased in the upper region of the IPS, but decreased in the lower region of the endocuticle. Calcium relative to carbon significantly increased in concentration only within the upper region of the prism over 32 days.

Although, there were few significant changes in concentration relative to carbon for the selected elements within the regions from 1-32 days, there were many significant changes in concentration during the smaller time intervals. The majority of the changes in element concentration relative to carbon occurred between 1-8 days, 8-16 days, and 16-32 days postecdysis (Table 2). Fewer changes in concentration occurred between 1-4 days and 4-8 days among the regions. Although, the EDE did not have significant changes in element content relative to carbon over 32 days, there was a significant drop in calcium between 4-8 days and then an increase of calcium at 16-32 days. The upper region of the IPS had numerous changes in element concentration relative to carbon within the smaller time intervals. There was a significant increase in calcium content between 1-8 and 8-16 days postecdysis and then the concentration decreased between 16-32 days. The phosphorus concentration dropped significantly between 16-32 days, despite the fact that it significantly increased over 32 days.

The middle region of the IPS stayed relatively constant in element composition with only the oxygen increasing between 1-4 days and the phosphorus decreasing between 16-32 days (Table 2). The lower region of the IPS did not have any significant changes relative to carbon (Table 2). The lower region of the IPS did not have any significant changes relative to carbon over 32 days postecdysis but had a drop in calcium between 8-16 days and a highly significant decrease in oxygen between 8-32 days after ecdysis. The upper, middle, and lower regions of the prisms had most of their significant changes in element concentration relative to carbon between 8-16 and 16-32 days postecdysis (Table 2). Ultimately, calcium and oxygen increased over 32 days in the upper region of the prism despite their highly significant drop in concentrations between 16-32 days. The phosphorus content did not change significantly over 32 days but followed the same trend as calcium and oxygen increasing between 8-16 days and then decreasing between 16-32 days. The middle region of the prism did not have any significant element changes relative to carbon over 32 days. However, during the smaller time intervals, the concentrations of calcium and oxygen, as seen in the upper region of the prism, increased between 8-16 days and then significantly decreased between 16-32 days postecdysis. The phosphorus content dropped during the 16-32 day interval. The lower region of the prism did not have any overall significant changes but had a decrease in calcium and oxygen between 8-16 days and then a significant increase in oxygen content between 16-32 days.

The upper, middle, and lower regions of the endocuticle had more significant changes in element concentrations relative to carbon within the smaller time intervals than any other regions, and the majority of them occurred between 1-8 and 16-32 days postecdysis (Table 2). The upper region of the endocuticle had a significant increase in oxygen between 1-32 days. This region also increased in calcium content between 1-8 and 16-32 days and phosphorus

between 1-8 days. The middle region of the endocuticle did not have any significant changes in element concentration over 32 days postecdysis but varied in element content during the smaller time intervals. The calcium content in the middle region of the endocuticle decreased between 4-8 days but increased between 1-8 and 16-32 days. The oxygen concentration relative to carbon repeatedly decreased and then increased throughout the smaller time intervals. The phosphorus content significantly decreased between 1-4 days, 1-8 days and 16-32 days postecdysis, but surprisingly the change in concentration was not significant from 1-32 days. The lower region of the endocuticle had a significant decrease in phosphorus concentration over 32 days even though it increased in content between 16-32 days. The calcium concentration increased significantly between 8-16 and 16-32 days but was not significant overall. The oxygen content in the lower region of the endocuticle varied as in the middle region at the same time intervals. The EDE, the middle and lower regions of the IPS, and the lower region of the prism had the least amount of significant changes in element composition relative to carbon over time (Table 2). Finally, magnesium concentrations relative to carbon were also statistically analyzed for each of the regions at every time interval but never revealed any significant changes. Therefore, they were not included in Table 2.

Ratios of selected elements were plotted to visualize patterns among and between regions (Fig. 10). Phosphorus to calcium ratios were graphed for the ten regions examined over time (Fig. 10a). Values appeared to roughly fall into three groups. The highest ratios of phosphorus to calcium were found in the upper and middle regions of the IPS and the upper and middle regions of the prisms. The amount of phosphorus relative to calcium in these regions increased dramatically from 1-8 days and then leveled off between 16-32 days. The lower regions of the IPS and prism, the EDE, and the upper region of the endocuticle grouped in the middle for ratio

Fig. 10. Ratios of (a) phosphorus to calcium and (b) magnesium to calcium for the ten regions examined over 32 days postecdysis.

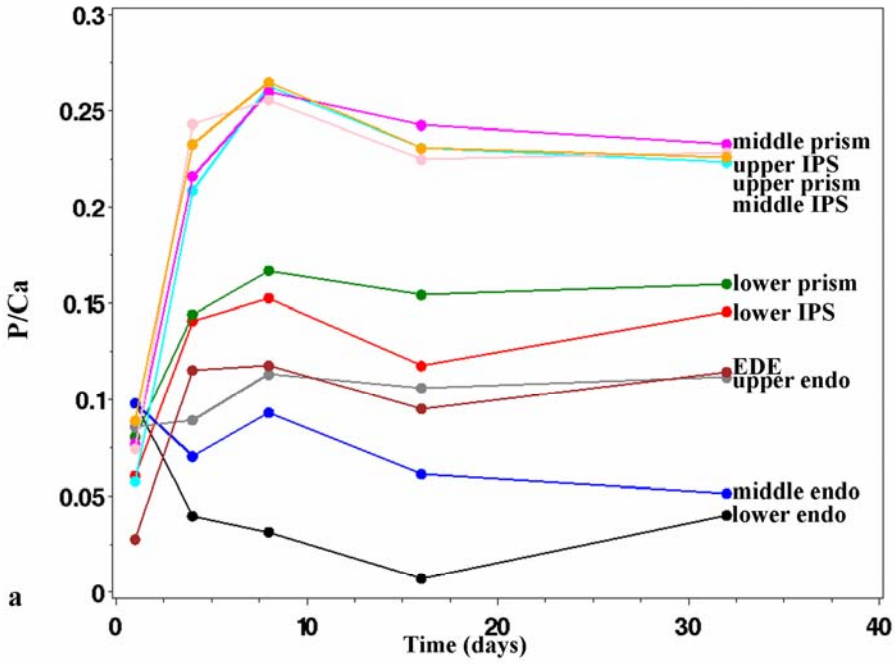
a
P/Ca
Time (days)
middle prism
upper IPS
upper prism
middle IPS
lower prism
lower IPS
EDE
upper endo
middle endo
lower endo

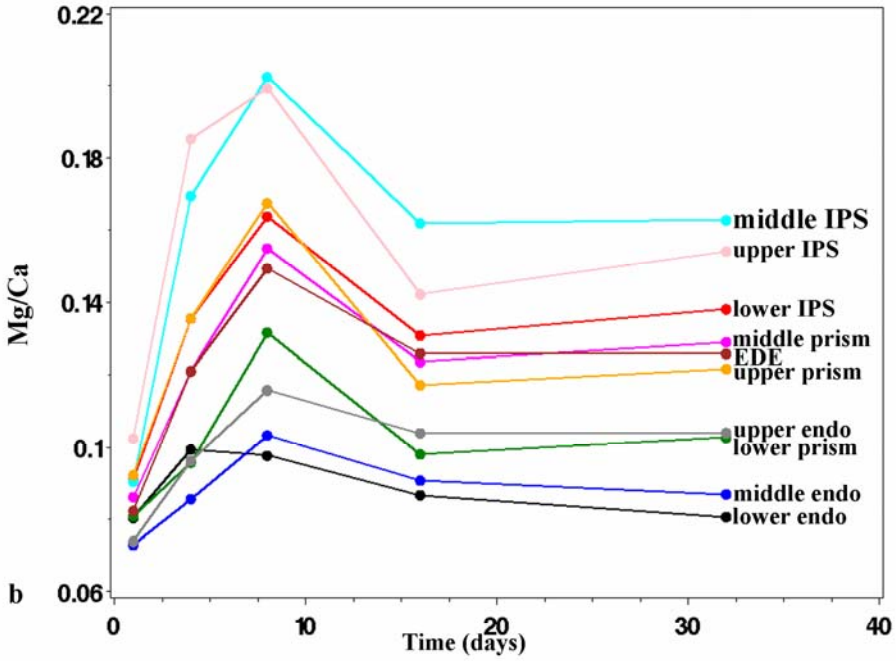
b
Mg/Ca
Time (days)
middle IPS
upper IPS
lower IPS
middle prism
EDE
upper prism
upper endo
lower prism
middle endo
lower endo

values relative to the other regions. The middle and lower regions of the endocuticle had the lowest ratios of phosphorus to calcium, varied little and decreased in concentration over time.

The magnesium to calcium ratios showed a more continuous group of values; however, some patterns were also seen (Fig. 10b). For example, the upper region of the IPS and middle region of the IPS had the highest phosphorus to calcium ratios and the highest magnesium to calcium ratios (cf. Fig. 10a, b). The lower region of the IPS, the middle region of the prism, the EDE, and the upper region of the prism were grouped in the middle of the ratios (Fig. 10b). The ratios for the top and middle groups increased from 1-8 days and then leveled off between 16 and 32 days postecdysis. The three regions of the endocuticle and the lower region of the prism had the lowest ratios of Mg/Ca and varied little or decreased over time.

The results from statistical tests compared concentrations of phosphorus, magnesium, calcium, and oxygen (atomic %) relative to carbon among regions over 1, 4, 8, 16, and 32 days postecdysis and are shown in Table 3. Among the ten regions, the comparison of the three regions of the IPS compared to the adjacent three regions of the prisms had one statistical difference in oxygen concentration. This suggested that the three regions of the IPS were similar to the three adjacent prism regions. The upper region of the endocuticle differed from the lower region of the endocuticle only by having a greater concentration of phosphorus at one day postecdysis. Otherwise, the regions of the endocuticle did not differ in element concentration over 32 days postecdysis and thus, were elementally similar. The upper and lower regions of the IPS had differences in phosphorus, calcium, and oxygen. The upper and middle and middle and lower regions of the IPS differed only in calcium and oxygen concentration. This suggested the upper and lower regions of the IPS had more differences than the upper and middle and middle

Table 3. Significant differences in relative concentrations for phosphorus, magnesium, calcium, and oxygen among regions over 1, 4, 8, 16, and 32 days postecdysis. The numbers represent the day at which there was a difference in concentration between regions. The greater than and less than symbols indicate the regions with the higher and lower concentrations. For example, the upperIPS had more phosphorus than the lowerIPS at 16 days postecdysis.

	Elements/Days			
Regional Comparisons	P	Mg	Ca	O
upperIPS vs. lowerIPS	16>		1>,16>	1>,16>
upperIPS vs. middleIPS			1>	1>, 16>
middleIPS vs. lowerIPS			16>	4<, 16>
upperprism vs. lowerprism	16>		4>, 16>	1>, 4>, 16>
upperprism vs. middleprism			16>	1>, 16>
middleprism vs. lowerprism			4<, 16>	1<, 8<, 16>
upperIPS vs. upperprism				16>
middleIPS vs. middleprism				
lowerIPS vs. lowerprism				
upperendo vs. lowerendo	1>			
upperendo vs. middleendo				
middleendo vs. lowerendo				
EDE vs. upperIPS	1>			1>, 16>
EDE vs. upperprism	1>, 16<		1>, 16>	1>, 16>
EDE vs. upperendo			1>,4>,16>,32>	1>,4>,16>
upperendo vs. upperIPS	1>,16<		1>,4>,16<,32<	1>,4>,16<
upperendo vs. upperprism	1>,16<	16<	1>,4>,16<,32>	1>,4>,16<
middleendo vs. middleIPS	1>,16<,32<		4>,16>	4>,16>
middleendo vs. middleprism	1>,16<,32<		4>,16>	4>,16>,32>
lowerendo vs. lowerIPS	1>			4>
lowerendo vs. lowerprism	1>			

and lower regions. Most of the differences among the regions of the IPS occurred at 1 and 16 days postecdysis, suggesting these regions differed at these times. The same trend was seen for the prisms. The upper and lower regions of the prisms had differences in three of the elements as compared to the upper and middle and middle and lower regions that only had differences in calcium and oxygen. This suggested that the upper and lower regions of the prism are more different than the upper and middle and middle and lower regions. The lower region of the endocuticle had few significant differences when compared to the lower regions of the IPS and prisms over time, suggesting their element concentrations were similar over 32 days postecdysis (Table 3).

The EDE had significant differences in two of the four elements when compared to the upper region of the IPS and the upper region of the endocuticle over time. The EDE had differences in phosphorus, calcium, and oxygen concentration relative to carbon in comparison to the upper region of the prism. This suggested that the EDE had more differences with the upper region of the prism, than the upper regions of the IPS and endocuticle. The regions that had the most significant differences in element concentration were the upper and middle regions of the endocuticle compared to the upper and middle regions of the IPS and prisms. There were significant differences in concentration for at least three of the four elements compared, and those differences existed at many time points. This suggests that these regions were quite different. Calcium and oxygen concentrations varied the most among regions, less with phosphorus concentration, and only one significant difference among the regions in magnesium concentration.

X-ray microanalysis was also used to re-examine three 32 day embedded samples after water treatment. Statistical analyses showed there were significant changes in element

concentration for only three of the ten regions after treatment (Tables 4a-b). In the EDE, the concentrations of calcium, phosphorus, oxygen, and magnesium relative to carbon all significantly decreased after water treatment (Table 4a). In the upper region of the IPS, the calcium concentration significantly increased post-water treatment. The upper region of the prisms had a significant increase in phosphorus concentration relative to carbon after water treatment (Table 4b). There were no statistically significant changes in element composition relative to carbon in the middle and lower regions of the prisms or among the regions of the endocuticle at 32 days postecdysis due to water treatment, thus suggesting these regions had little or no soluble mineral.

Light Microscopy and SEM

Histological sections of eight-day cuticle had an exocuticle, an endocuticle, a hypodermis, but not a membranous layer (Fig. 11a). At 13 days postecdysis, the SE image of a fractured sample revealed an endocuticle that had stacks of lamellae with fibers intertwined and a membranous layer (Fig. 11b). The membranous layer appeared as thin layers of lamellae that were horizontal to the cuticle surface. The presence of the membranous layer suggests that intermolt has begun by 13 days postecdysis. The light microscope images taken from 16- and 32-day cuticles each had an exocuticle, a thick endocuticle, and a membranous layer (cf. Fig. 11c-d). A portion of the hypodermis was visible underneath the membranous layer. It appeared that the 32-day cuticle had a thicker membranous layer with more horizontal layers than the 16-day cuticle.

Table 4a. Changes in element composition relative to carbon after water treatment for regions of the epicuticle and distal exocuticle (EDE) and the IPS at 32 days postecdysis. The mean relative concentrations (atomic %) are shown for the untreated and treated cuticle as well as the statistical analyses. The significant difference was $p \leq 0.0125$ and denoted by *. The highly significant difference, $p \leq 0.0001$, was denoted by †.

		Mean Concentrations		Change	
Regions	Elements	Dry %	Wet %	(Wet-Dry%)	p-value
EDE	Ca	16.43	16.15	-0.28*	0.0002
	P	1.86	0.78	-1.08†	0.0001
	O	43.48	36.27	-7.21*	0.0017
	Mg	2.03	1.96	-0.07*	0.0067
upper IPS	Ca	11.78	16.61	4.83*	0.0008
	P	2.61	2.55	-0.06	0.6818
	O	30.70	37.39	6.69	0.0201
	Mg	1.68	2.02	0.34	0.1692
middle IPS	Ca	8.22	11.01	2.79	0.7148
	P	1.85	3.07	1.22	0.2677
	O	23.53	22.04	-1.49	0.7800
	Mg	1.25	1.45	0.20	0.7032
lower IPS	Ca	6.92	7.39	0.47	0.2152
	P	1.02	1.57	0.55	0.8989
	O	20.71	13.71	-7.00	0.4608
	Mg	0.92	0.76	-0.16	0.3671

Table 4b. Changes in element composition relative to carbon after water treatment for regions of the prism and endocuticle at 32 days postecdysis. The mean relative concentrations (atomic %) are shown for untreated and treated cuticle as well as the statistical analyses.

		Mean Concentrations		Change	
Regions	Elements	Dry %	Wet %	(Wet-Dry%)	p-value
upper prism	Ca	9.72	17.08	7.36	0.8287
	P	2.14	4.27	2.13*	0.0005
	O	22.89	30.01	7.12	0.9901
	Mg	1.08	1.92	0.84	0.7640
middle prism	Ca	6.48	11.07	4.59	0.9106
	P	1.51	3.03	1.52	0.0170
	O	17.83	21.28	3.45	0.9686
	Mg	0.81	1.32	0.51	0.9504
lower prism	Ca	5.28	4.68	-0.60	0.4818
	P	0.86	1.12	0.26	0.8611
	O	13.35	13.29	-0.06	0.4830
	Mg	0.50	0.50	0.00	0.9667
upper endo	Ca	11.01	11.85	0.84	0.0605
	P	1.21	1.93	0.72	0.8707
	O	31.75	18.93	-12.82	0.3693
	Mg	1.12	1.03	-0.09	0.4152
middle endo	Ca	12.82	14.07	1.25	0.0970
	P	0.65	1.11	0.46	0.9940
	O	34.65	20.78	-13.87	0.3877
	Mg	1.07	1.01	- 0.06	0.4087
lower endo	Ca	11.66	11.54	-0.12	0.0860
	P	0.46	0.84	0.38	0.8722
	O	31.90	18.30	-13.60	0.2407
	Mg	0.92	0.92	0.00	0.4535

Fig. 11. Light microscope (a, c-d) and secondary electron (b) images of the cuticle showing the presence of a membranous layer by 13 days postecdysis. a: An eight-day cuticle showing an exocuticle (ex), an endocuticle (en), a hypodermis (hy), but not a membranous layer (arrow). b: A SE image of 13 day fractured cuticle displaying an endocuticle (en) that has stacks of lamellae with fibers intertwined and a membranous layer (ml). The membranous layer has thin lamellae horizontal to the cuticle surface. c-d: Light microscope images of 16- and 32-day cuticles showing an exocuticle, a thick endocuticle, and a membranous layer (arrow).

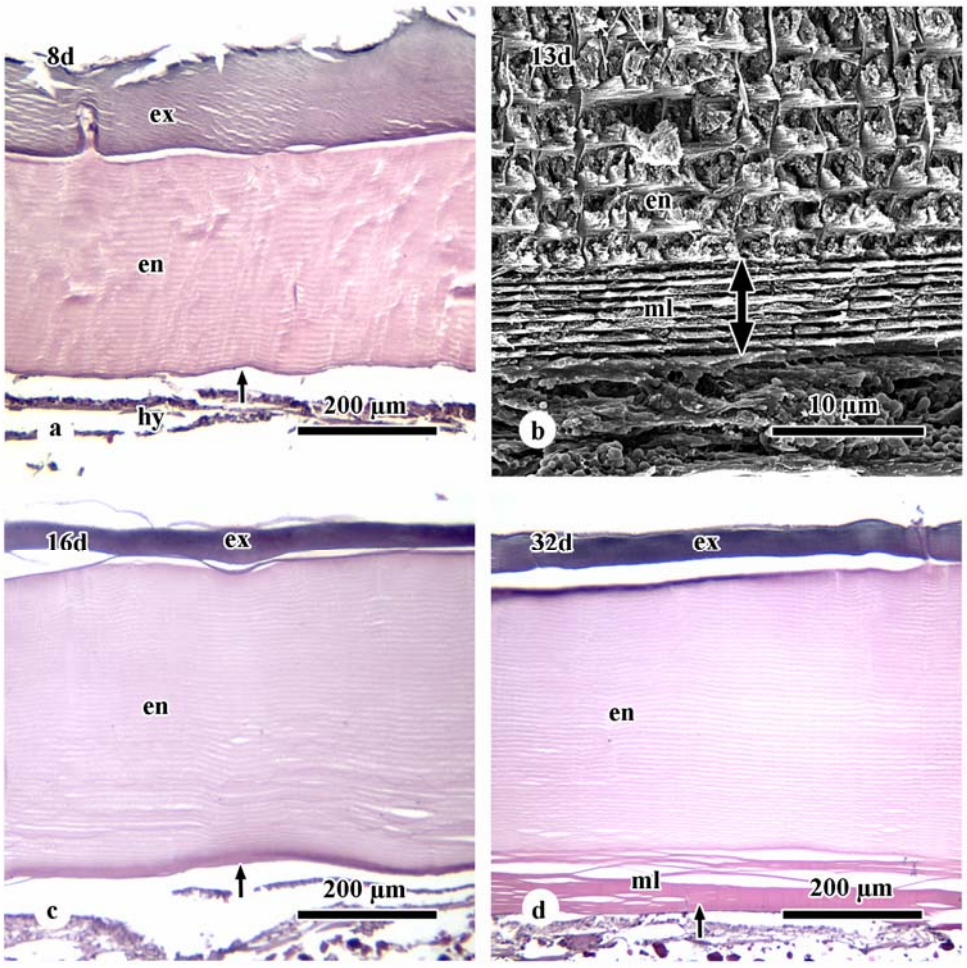
8d
ex
en
hy
200 µm
a
13d
en
ml
10 µm
b
16d
ex
en
200 µm
c
32d
ex
en
ml
200 µm
d

DISCUSSION

The present investigation revealed the mineralization pattern, the mineral phases, and elemental composition of the dorsal carapace cuticle of the blue crab during postecdysis (1, 4, and 8 days) and intermolt (16 and 32 days) stages. This study adds information to Hequembourg's (2002) observations to give an extended description of the calcium carbonate deposition pattern in the dorsal carapace of *Callinectes sapidus* throughout the molt cycle (D_2-32 days postecdysis). Hequembourg (2002) documented soluble mineral in the epi/exocuticle border and the IPS at 12 and 24 hours postecdysis. This study localized where soluble mineral occurred in the cuticle and determined when it transformed to a less soluble, crystalline mineral over 32 days postecdysis. This study supports and documents the presence of amorphous mineral, presumably ACC or ACP in the various regions of the crab cuticle. For most regions within the cuticle, the amorphous mineral transformed to a less soluble form, presumably calcite or calcium phosphate, in a predictable spatial and temporal pattern. X-ray microanalysis showed that significant changes in element concentrations relative to carbon occurred within and among the regions of the cuticle over 32 days postecdysis. The P/Ca and Mg/Ca ratios also varied among the regions. Finally, statistical analyses revealed that there were three elementally distinct regions within the cuticle: the EDE, the exocuticle, and the endocuticle.

Hypotheses were proposed and tested using the SEM to determine the mineralization pattern and elemental composition of the dorso branchial cuticle of the blue crab during postecdysis and intermolt. The first null hypothesis states that amorphous mineral is not present in the cuticle. If amorphous mineral is present in the cuticle then it would be highly soluble and removed by water treatment. The second null hypothesis proposed that amorphous mineral in the cuticle does not transform to a less soluble polymorph in a predictable spatial and temporal

pattern during postecdysis. If the mineral is amorphous and transforms to a crystalline mineral phase in a predictable fashion then, soluble mineral would become less soluble over time. Both of these hypotheses were tested by comparing BSE images of the cuticle before and after water treatment at 1, 4, 8, 16, and 32 days postecdysis. BSE images after water treatment revealed that there was soluble mineral in the cuticle and with time it became less soluble in most regions. Therefore, it is suggested that amorphous mineral was present and transformed to a crystalline mineral phase for most of the regions over 32 days postecdysis, thus the first two null hypotheses were rejected. These results were expected considering that amorphous mineral had already been observed in the crab cuticle at early time periods and calcite has been documented as the mineral phase at intermolt (Vinogradov, 1953; Hegdahl et al., 1977a,b; Hequembourg, 2002; Dillaman et al., 2005).

The first region examined before and after water treatment was the EDE that consists of a bilaminar epicuticle and the distal portion of the exocuticle (Drach, 1939; Compère, 1995). The epicuticle is composed of calcite crystals but not lamellae (Drach, 1939). The mineral in the epicuticle has previously been described as aggregates of crystalline mineral that vary in shape and size and reach toward the outer border but end just short of the surface (Drach, 1939; Hegdahl et al., 1977b). This description of the mineral fits the morphology of crystals seen in the high magnification images of the EDE at four days postecdysis (Fig. 7). The results from comparing BSE images of before and after water treatment revealed that the EDE in the embedded and fractured samples had a less soluble or crystalline mineral phase that did not appear to change from 1-32 days postecdysis (cf. Figs. 3, 4, 6, and 8).

The external zone (Drach, 1939; Hegdahl et al., 1977a; Modla, 2006) or the epicuticle/exocuticle border (Dillaman et al., 2005) has been documented as a highly mineralized

area in the exocuticle where prisms are not present. It has been suggested that the mineral that fills the external zone and the IPS is the same as the mineral in the epicuticle and is crystalline at intermolt (Drach, 1939; Hegdahl et al., 1977a). Hegdahl et al. (1977a) states that the external zone may have been previously regarded as a separate and different zone but infers that it is not. A more recent investigation disagreed and suggested that the external zone in the cuticle of *Callinectes sapidus* was different than other regions (Modla, 2006). The external zone and the IPS were the only regions that stained when fixed with uranyl acetate suggesting that these regions had a high affinity to molecules rich in phosphates, to cationic and anionic proteins, and to carbonate ions, unlike the other regions in the cuticle. In this investigation, the BSE images documented a unique mineralization pattern in the proximal external zone compared to other regions within the cuticle over time, which was consistent with Modla's (2006) observations (cf. Figs. 3b2, 3c2, 6b2, 6c2). The external zone had an extensive void after water treatment until 16 days postecdysis when the mineral was crystalline and extended down into the upper IPS margins (cf. Figs. 3c3, 4a3, 4b3, 6c2, 8a2, 8b2). In an earlier study of *Cancer pagurus*, results also suggested that the mineral in the IPS was an extension from the external zone (Hegdahl et al., 1977a).

The exocuticle is composed of the IPS and prisms. Mineral deposition occurs in the exocuticle matrix within the pore canals, between the chitin-protein fibers, and embedded in the fibers (Hegdahl et al., 1977a). X-ray diffraction has shown that the majority of mineral in the exocuticle of *Cancer pagurus* at intermolt is calcite, but it is unevenly distributed (Hegdahl et al., 1977a). The IPS is one of the initial sites of mineral deposition (Giraud-Guille, 1984). The IPS contains cation-binding glycoproteins that have an affinity for calcium as well as carbonic anahydrase that catalizes the conversion of CO_2 into bicarbonate (Roer and Dillaman, 1993).

Early postecdysial alterations have been shown to occur in the glycoproteins of the IPS but not in the prisms (Tweedie et al., 2004). This suggests that the glycoproteins in the IPS control the pattern of mineralization in the exocuticle. The mineral in the IPS has been described as aggregates of crystals in well-mineralized areas but occurs as small plate-like crystals in poorly mineralized portions (Hegdahl, 1977a).

In a previous study on *Callinectes sapidus*, it was suggested that the mineral in the IPS was amorphous that later transformed to calcite (Hequembourg, 2002). However, the results from this study disagreed with Hequembourg's generalized assumption and provided new and detailed insight into the mineralization pattern of the IPS during postecdysis. In this investigation, the amorphous mineral in the IPS was documented, but transformation of the mineral phase only occurred in the upper region of the IPS. Specifically, the upper, middle, and lower regions of the IPS initially had amorphous mineral at one day postecdysis (cf. Figs. 3a2, 6a2). At eight days, the crystalline mineral from the epicuticle fills in the upper region of the IPS and extended further down into the upper portion of the IPS until 32 days postecdysis (cf. Figs. 3c3, 4a3, 4b3, 8b2). The mineral in the middle and lower regions of the IPS did not transform to a less soluble mineral, but remained amorphous (cf. Fig. 4b2-3). This pattern of calcium carbonate deposition differed from other regions in the cuticle and suggested that nucleation sites or proteins in the IPS were site-specific. This initial deposition of amorphous mineral, presumably ACC, forms honeycomb-shaped IPS in the exocuticle that quickly makes the cuticle rigid with minimal calcification (Compère et al., 1993, Dillaman et al., 2005). In the BSE images of the fractured samples after water treatment, the mineral in the middle and lower regions of the IPS appeared less soluble from 8 -32 days postecdysis than in the embedded samples (cf. Figs. 6c2, 8b2). The fractured samples were used for identifying certain features of

the cuticle and visualizing the crystal morphology of the mineral but may have led to unreliable observations of the mineral phases due to step-wise fracturing in which the layers are not fractured perpendicular to the surface at all levels.

The prisms are polygonal in shape and extend from the epicuticle to the endocuticle (Hegdahl et al., 1977a). The prisms fill in with mineral uni-directionally from the epicuticle to the endocuticle, not bi-directionally like the IPS (Hequembourg, 2002). In this study, the mineral starts to fill in the prisms between one and four days postecdysis. The mineral in the upper region of the prisms appeared to be less soluble than the mineral in the middle and lower regions of the prisms at four and eight days postecdysis (cf. Figs. 3b2, 6b2). Consequently, it is suggested that the upper regions of the prisms contained mostly crystalline mineral by four or eight days postecydsis with minor amounts of amorphous mineral, while the middle and lower regions of the prisms contained a mixture of amorphous and crystalline mineral phases from 4-16 days (cf. Figs. 3b2, 3c2, 4a2, 6b2, 6c2, 8a2). At 32 days postecdysis, the mineral in the prisms, except the lower region of the prisms, had completely transformed to a crystalline mineral, presumably calcite (cf. Figs. 4b2, 8b2). This pattern of depositing a mixture of mineral phases within the cuticle was also observed and documented in the spicules of *Strongylocentrotus purpuratus.* The spicules had a mixture of 50% ACC and calcite that co-existed initially and later transformed to a fully crystalline polymorph (Raz et al., 2003). The mineral in the proximal portion of the lower region of the prisms did not undergo complete transformation to calcite because, surprisingly, this area of the cuticle never filled in with mineral and remained unmineralized at 32 days postecdysis (cf. Figs. 4b2, 8b2). This observation was consistent with a previous study that found the lower regions of the prisms were poorly mineralized at intermolt in *Cancer pagurus* (Hegdahl et al., 1977a). The lack of mineral deposited in the lower region of

the prisms can be explained by this region being one of the last layers mineralized during postecdysis. The distance that calcium has to be transported to reach the lower region of the prisms increases during postecdysis and therefore may slow the rate of calcification. Also, the pore canals may be completely degraded before the onset of mineralization in the lower region of the prisms. This would not allow transport of ions from the hypodermis to the cuticular layer and thus prevent deposition of mineral in this region (Roer and Dillaman, 1984).

The endocuticle comprises approximately 75% of the whole cuticle (Hegdahl et al., 1977c). The thick endocuticle is made of lamellae and numerous elliptical shaped pore canals that contain fibers and small crystals (Hegdahl et al., 1977c). The fibers in the lamellae of the endocuticle are contained in tubes and aligned with calcite mineral to form long rod-shaped elements (Hegdahl et al., 1977c; Roer and Dillaman, 1984). X-ray diffraction patterns from the cuticle of *Cancer pagurus* have shown that calcite is present in the endocuticle at intermolt (Hegdahl et al., 1977c). Early researchers assumed that the mineral in the endocuticle was calcite and homogeneous due to the fact this region is calcified as it is deposited (Drach, 1939; Roer and Dillaman, 1984). However, one study stated that the endocuticle was not homogeneously mineralized but had a variation in mineral (Hegdahl et al., 1977c). The results from water treatment in this study, agreed with Hegdahl's observation. The endocuticle had both mineral phases (soluble and less soluble) from 1-32 days where it then, appeared to be composed entirely of crystalline mineral (Fig. 5).

The location of the amorphous mineral in the endocuticle appeared in the BSE images post-water treatment as obvious holes that were organized into horizontal rows evenly spaced among the cuticle. The holes were described previously by Hegdahl et al. (1977c) as "continuous walls around electron lucent openings" and suggested that these openings in the

native state of the tissue contained fibers. In a recent study, it has also been shown that quick-freezing in liquid nitrogen and the process of lyophilization creates tunnels or holes (due to inadequate freezing and displacement of fibers by ice) where fibers once appeared in the crab cuticle (Modla, 2006). The holes observed in this study could be a result of the way the tissue was processed. However, the fact that the holes appeared only after water treatment implied that amorphous mineral existed in the holes or tubes that contained fibers. This study suggests that the crab does not transform the small amounts of amorphous mineral in the tubes until later time intervals, because any transformation from hydrated, soluble salts to dehydrated and less soluble minerals requires energy and time (Simkiss, 1994). The hypodermis is expending energy transporting ions and calcifying the pre-exuvial layers at the same time that it is depositing the endocuticle matrix and calcifiying it during postecdysis.

The third null hypothesis states that the concentrations (atomic %) of calcium, magnesium, phosphorus, and oxygen relative to carbon and the ratios of certain elements do not change within regions of the cuticle over time. If the relative concentrations of selected elements are changing over time, then the mineral composition may also be changing during postecdysis. To test this hypothesis, x-ray microanalysis was performed on the samples using the SEM. The relative concentrations for the selected elements increased for most regions over time, suggesting change is occurring and that mineral is accumulating within the cuticle after ecdysis (Table 1a-d). The statistical analyses of the quantitative data from x-ray microanalysis showed that the concentrations (atomic %) of calcium, magnesium, phosphorus, and oxygen relative to carbon and the ratios of certain elements did change within some of the regions of the cuticle over time, thus rejecting the third null hypothesis. Specifically, the upper regions of the IPS and prisms and

the upper and lower regions of the endocuticle had significant changes in element concentration relative to carbon over 32 days postecdysis.

In this investigation, the EDE did not display significant changes in element concentrations relative to carbon over 32 days postecdysis (Table 2). This suggests that the initial mineral did not transform or change over time, as was also seen in the BSE images of the cuticle before and after water treatment. Alternatively, the upper region of the IPS significantly increased in phosphorus and oxygen content over 32 days, while increasing in calcium during smaller time intervals. These results and the results from the BSE images after water treatment suggest that the mineral phase in the upper region of the IPS initially is mineralized with amorphous mineral that transforms over time to a crystalline polymorph. Since there was a significant increase in phosphorus and oxygen concentrations relative to carbon over time in the upper region of the IPS, it is suggested that the mineral may be composed of ACC and ACP that transformed to $Ca_3(PO_4)_2$ or calcite by 32 days postecdysis. This is consistent with a previous study that showed the mineral in the cuticle is comprised mostly of $CaCO_3$ with small amounts of $Ca_3(PO_4)_2$ (Dalingwater and Mutvei, 1990).

Alternatively, the middle and lower regions of the IPS did not change in element composition relative to carbon over 32 days postecdysis and had very few changes in element concentration within the smaller time intervals. This suggested that the mineral phase in these regions was relatively stable. The combined results from the x-ray microanalysis and the BSE images after water treatment suggest that the mineral phase in the middle and lower regions of the IPS was initially amorphous mineral and that it did not change over time. The mineralization pattern and mineral phases in the upper region of the prisms may have differed from the middle and lower regions because there is a higher proportion of glycoproteins in the upper region of the

IPS than in the lower region (Giraud-Guille, 1984) and it has been suggested that glycoproteins can regulate mineralization (Tweedie et al., 2004).

The upper regions of the prisms had significant increases in calcium and oxygen concentrations relative to carbon over 32 days, suggesting that the mineral was mostly $CaCO_3$. Most of the changes in element concentration occurred between 8-16 days and 16-32 days suggesting that most of the mineral was deposited and transformed between 8-32 days postecdysis. This pattern of mineral deposition was also observed in the water treated BSE images (cf. Figs. 3c2, 4a2, 4b2, 6c2, 8b2). The middle and lower regions of the prism did not significantly change in element composition over 32 days, but changed during the smaller time intervals. This suggests that the mineral phase in these regions does not change significantly over 32 days, but may undergo significant fluctuations over shorter time intervals. Since there was an increase in calcium and oxygen over time, it is suggested that the initial mineral in the prisms was ACC or ACP and that transformation to $CaCO_3$ occurred with time.

The upper region of the endocuticle had a significant increase in oxygen relative to carbon over 32 days and changes in phosphorus and calcium concentrations occurred between 1-8 days and 8-16 days. These changes in element concentrations suggest that the mineral may be comprised of ACC, ACP, $CaCO_3$, $Ca_3(PO_4)_2$, or a mixture. The significant increase in oxygen suggested that the mineral was transformed to calcite or calcium phosphate over 32 days postecdysis. The middle region of the endocuticle had numerous changes in element concentration during smaller time intervals but no significant changes over 32 days. This may be explained by the sampling method. The location of measurements taken for the middle and lower regions changed as the cuticle became thicker over time. For example, at the beginning of the study the measurement for the middle region of the endocuticle was taken at random in the

middle of the endocuticle, but by the end of the study this same spot would be considered the upper region of the endocuticle. Therefore, the middle and lower regions of the endocuticle are misrepresented and most likely follow the same mineralization pattern as the upper region of the endocuticle. However, x-ray microanalysis showed that the lower region of the endocuticle had a significant change in phosphorus content over 32 days and changes in calcium and oxygen during the smaller time intervals, but this again suggests that the endocuticle is mineralized by ACC or ACP that changes to $CaCO_3$ with small amounts of $Ca_3(PO_4)_2$ over time.

The second part of the third null hypothesis states that the ratios of certain elements do not differ among the regions of the cuticle. The graphs that showed the ratios of phosphorus to calcium and magnesium to calcium revealed that the values varied within and among regions over time (Fig. 10a-b), thus rejecting the third null hypothesis. These results are expected if the mineral phases differ among regions and if transformation occurs in some regions, but not all. As defined by Levi-Kalisman et al. (2000), ACC should have a higher amount of magnesium and phosphorus than the crystalline mineral phases. Therefore, the ratios (P/Ca and Mg/Ca) should be higher in the ACC than in the crystalline mineral, presumably calcite and can be correlated to solubility (Priester et al., 2005). In this study, the upper and middle regions of the IPS and prisms had the highest P/Ca ratios compared to the other regions in the cuticle. As expected they contained soluble mineral in the BSE images after water treatment in earlier time intervals, and then some of these regions transformed to a crystalline mineral. The graph of Mg/Ca showed that the upper, middle, and lower regions of the IPS had the highest values. This was expected because the BSE images after water treatment showed that the mineral in the IPS was soluble or amorphous. Only the upper region of the IPS transformed to a less soluble mineral between 8-16 days, which was when there was a drop in the ratios, as compared to a dramatic increase in ratios

between 1-8 days. Different relative concentrations of magnesium ions have also been found in the IPS of *Carcinus maenas* after ecdysis (Compère et al., 1993). In *Callinectes sapidus*, the mineral in the middle and lower regions of the IPS remained amorphous but was stable over time. Becker et al. (2005) showed that with increased Mg:Ca ratios the deposited ACC was more stable. The EDE was ranked in the middle for concentrations of phosphorus and magnesium when compared to the other regions and appeared as a less soluble or crystalline mineral in all BSE images. The regions of the endocuticle had the lowest values for P/Ca and Mg/Ca ratios and were composed mostly of crystalline mineral with small traces of amorphous mineral as seen in the BSE images after water treatment. The P/Ca and Mg/Ca ratios increased dramatically in value for most regions between 1 and 8 days and then leveled off. This can be explained by previous research that showed mineralization proceeds at an extremely rapid rate in the cuticle until 7-8 days postecdysis (Travis, 1957; Cameron, 1985).

The fourth null hypothesis states that regions of the dorsal carapace cuticle did not differ in element composition during postecdysis and intermolt stages. Therefore, it was tested using x-ray microanalysis. Statistical analyses of the results revealed that element composition differed among regions of cuticle in the dorsal carapace, thus the fourth null hypothesis was rejected. The results from x-ray microanalysis showed there were three elementally distinct regions within the cuticle: the EDE, the exocuticle, and the endocuticle (Table 3). In the past, these three regions have been differentiated due to their morphological characteristics, time of development, and composition. Morphologically, the epicuticle has two layers with vertical fibers and is composed of lipoproteins and calcium salts (Travis, 1965). The exocuticle and endocuticle are composed of chitin-protein matrices that form lamellae that are embedded with mineral. Deposition of the epicuticle and exocuticle occurs before the molt, while the

endocuticle is deposited after ecdysis. The epicuticle and exocuticle are tanned and calcified, while the endocuticle is hardened only by calcium (Roer and Dillaman, 1984). In protein composition, the exocuticle contains numerous glycoproteins that change expression over the molt cycle, while the endocuticle is composed of less glycoproteins and remains constant in expression (Marlowe et al., 1994; Welinder, 1975). In this investigation, x-ray microanalysis revealed that the EDE differed from the IPS, the prisms, and the endocuticle. The adjacent regions of the IPS and prism regions were similar in element composition over time, suggesting that the exocuticle region is relatively homogeneous laterally, but not vertically, in mineral. The regions of the endocuticle were similar in element composition over 32 days postecdysis. However, there were some unexpected results that showed the lower regions of the IPS and prisms (proximal exocuticle) were similar in element composition to the lower endocuticle. This may be explained by the fact that these regions are deposited at different times but are mineralized around the same time during postecydsis. The lower regions of the IPS and prisms are the last portion of the cuticle deposited during pre-ecdysis, just as the lower endocuticle is the last tissue deposited in postecdysis. After ecdysis, the lower regions of the prisms and the endocuticle are the last regions to be calcified, and that may be why they have similar content. They may not be fully calcified by the time the pore canals degrade.

The final hypothesis states that the intermolt cuticle treated with water differs in element composition from the untreated cuticle. To test this, x-ray microanalysis was performed on three 32 day samples before and after water treatment and compared statistically. The statistical results from x-ray microanalysis conducted on 32 day cuticles before and after water treatment revealed that three of the ten cuticular regions had a different element composition after treatment with water. The EDE decreased significantly in relative concentrations of phosphorus,

oxygen, magnesium, and calcium post-water treatment, suggesting there was some soluble mineral in this region. These results were unexpected and surprising because, the BSE images of this region after water treatment suggested that the mineral in the EDE was not soluble. The amorphous mineral was not identified in the BSE images and without re-examination of the samples after water treatment using x-ray microanalysis the assumption would have been that the EDE region had only crystalline mineral. The results from both of the techniques combined suggest that the EDE had both a stable amorphous mineral phase and a crystalline polymorph at 32 days postecdysis. This demonstrated that both techniques are needed to confirm all the mineral phases. It would be ideal to re-examine all water treated embedded samples for all time intervals using x-ray microanalysis, but this was not done in this study due to time constraints.

Another region that had a change in element composition after water treatment was the upper region of the IPS with a significant increase in calcium concentration, with a necessary decline in phosphorus and carbon. This may suggest that the mineral in the upper region of the IPS was mostly calcite with small amounts of ACP. The water treatment would have removed the ACP, thus decreasing the phosphorus concentration. The calcite mineral would have remained in the region after water treatment and caused the analysis of before and after water treatment to show an increase in calcium. This change in concentration can be also explained by the fact that this data is presented as percents and the change in one element effects another. Another explanation of why the calcium increased in the upper region of the IPS after water treatment may be that the carbon content decreased as a result of soluble proteins or sugars in the matrix being washed out by the addition of water which caused an increase in the calcium concentration. The same explanation can be applied to the decrease in carbon content revealed in the upper region of the prism that caused the data to imply that there was a significant increase

in phosphorus after water treatment. Alternatively, the mineral in the upper region of the prism at 32 days postecdysis is composed of ACC, $CaCO_3$, and small amounts of $Ca_3(PO_4)_2$ and water treatment may have removed ACC leaving behind calcite and calcium phosphate. As a consequence, the statistical analysis before and after treatment showed an increase in phosphorus. Since these elements are percents there was a decrease in the carbon content.

ACC has been found in many organisms. Of known biominerals 80% are crystalline while 20% are amorphous (Lowenstam and Weiner, 1989). Amorphous minerals are random networks of bonds, rather than periodic structures (Addadi et al., 2003). This disorder in the lattice structure causes amorphous minerals to have a high solubility (Simkiss, 1994; Levi-Kalisman et al., 2000; Becker, 2003). Crustaceans use this soluble ACC as storage deposits for fast dissolution and mobilization of ions during the molt cycle (Addadi et al., 2003; Greenaway, 1983). Amorphous minerals also have isotropic properties that facilitate equal distribution of stress among the crystal faces and are easier to mold into structures or shapes (Simkiss, 1994; Levi-Kalisman et al., 2000). The sponge *Clathrina* sp. uses ACC to form spicules (Aizenberg et al., 1996). Many organisms also use amorphous mineral as a precursor phase to a crystalline polymorph. An example is the blue crab that uses ACC to stiffen its exoskeleton quickly after ecdysis for survival, before transforming the mineral to a crystalline polymorph, presumably calcite (Hequembourg, 2002). Amorphous calcium carbonate contains one water molecule per calcium carbonate, but the transient forms do not contain water and resemble the crystalline form in structure (Addadi et al., 2003).

It has been shown that ACC and ACP transform to a crystalline mineral in uncontrolled environments that are thermodynamically and kinetically favored unless stabilized by macromolecules or ions (Levi-Kalisman et al., 2000). Macromolecules that occur in conjunction

with ACC are glycoproteins rich in glutamic acid, while proteins associated with calcite are high in aspartate acids (Aizenberg et al., 2002). In tunic spicules, high amounts of magnesium were suggested to be important in regulating different calcium carbonate phases (Aizenberg et al., 2002). In a more recent study, it was confirmed that magnesium ions stabilize the ACC by slowing the transformation to a crystalline phase and thus provides a mechanism for controlling crystal morphology (Loste et al., 2003). Transformation of ACC occurs due to a solid-solid state rearrangement of the atoms of the mineral to form crystalline material (Addadi et al., 2003). Finally, amorphous polymorphs are more stable with increasing pH while crystalline mineral becomes less stable (Simkiss, 1994).

In this investigation, soluble and non-soluble mineral phases were documented in the dorso branchial cuticle of *Callinectes sapidus* at late postecdysis and intermolt stages.
The next step in understanding the mineralization process of the blue crab cuticle should be to identify the mineral that occurred in the ten regions examined in this study over the same time intervals using infrared spectroscopy. This analysis technique would identify the mineral phases (amorphous calcium carbonate, amorphous calcium phosphate, calcium phosphate, high-Mg calcite, and calcite) and provide a more detailed understanding of transformation of the mineral that was suggested in this study. Infrared spectroscopy is the most valuable technique for biomineralization studies according to Lowenstam and Weiner (1989). The infrared spectra can identify both crystalline and amorphous minerals even when they occur in the same sample by the number of peaks and their location (Addadi et al., 2003). However, the identification of ACC in a specimen using infrared spectroscopy requires grinding up the entire cuticle and gives bulk estimates that limit the ability to localize the mineral phase within a region over time, making the results from this study important in determining the spatial pattern of mineralization

within the cuticle. Other methods that have been used to identify amorphous minerals are: x-ray absorption spectroscopy, thermogravimetry, and elemental analysis by atomic absorption spectroscopy (Becker et al., 2003).

In summary, results from the BSE images and x-ray microanalysis suggested that there was amorphous mineral presumably, ACC or ACP in the cuticle. Over 32 days postecdysis, the mineral transforms to a crystalline form, presumably calcite and/or calcium phosphate in most regions (Table 5). The amorphous mineral was found in the proximal portion of the external zone, the upper, middle, and lower regions of the IPS, the upper, middle, and lower regions of the prisms, and small amounts in the EDE and the endocuticle. The external zone and upper region of the IPS had amorphous mineral initially that transformed to a crystalline mineral between 8-32 days postecdysis (Table 5). The upper region of the IPS also changed in element composition over time. However, the middle and lower regions of the IPS remained amorphous or soluble throughout the 32 days postecdysis and the element composition did not change with time. A composite of both amorphous and crystalline mineral was found in the regions of the prisms until 32 days postecdysis where it then appeared to have only crystalline mineral, presumably calcite. The element concentrations for the upper region of the prisms did change over 32 days, while the middle and lower regions of the prisms only had changes in concentration during smaller time intervals. The EDE had mainly crystalline mineral, but had small amounts of amorphous mineral at 32 days, suggesting this layer is made of a composite mineral that does not change with time. The x-ray microanalysis data supported this conclusion by showing there was no change in element concentrations over time in this region. The endocuticle had the majority of mineral as crystalline but appeared to transform small traces of amorphous mineral into less soluble mineral between 16-32 days postecdysis. This was also

Table 5. Mineral phases within the regions of the cuticle during postecdysis.

Regions	Mineral phases over time
EDE	composite of amorphous and crystalline mineral from 1-32 days
upper IPS	amorphous mineral transforms to a crystalline mineral phase between 8-32 days postecdysis
middle IPS	amorphous mineral only and does not transform over time
lower IPS	amorphous mineral only and does not transform over time
upper prism	a composite of amorphous and crystalline mineral that transforms to a crystalline polymorph between 8-32 days
middle prism	a composite of amorphous and crystalline mineral that transforms to a crystalline polymorph between 16-32 days postecdysis
lower prism	never completely mineralizes, but some of the mineral present is amorphous from eight days on
upper endo	the majority of the mineral is crystalline, but has small, localized areas that contain amorphous mineral that transforms to a crystalline mineral phase between 16-32 days postecdysis
middle endo	the majority of the mineral is crystalline, but has small, localized areas that contain amorphous mineral that transforms to a crystalline mineral phase between 16-32 days postecdysis
lower endo	the majority of the mineral is crystalline, but has small, localized areas that contain amorphous mineral that transforms to a crystalline mineral phase between 16-32 days postecdysis

seen in the x-ray microanalysis data that showed the upper and lower regions of the endocuticle had changes in element composition over time. These patterns of mineral deposition have also been observed in other crustacean studies. One example is a study on the mineral composition of the exoskeleton of a crayfish *Procambarus clarkii* that showed ACC and calcite co-exists in the exoskeleton (Travis, 1963; Sugawara et al., 2006). Interestingly, another study using infrared spectroscopy and x-ray diffraction analysis on the giant prawn *Macrobrachium rosenbergii* over 30 days postecdysis had similar results to this study. The mineral in the exoskeleton was composed initially of ACC and ACP and was partially transformed to calcite over 30 days postecdysis (Soejoko and Tjia, 2003).

This present investigation is important because it has documented the mineralization pattern for ten regions within the blue crab cuticle during postecdysial and intermolt stages. New observations included the discovery that the middle and lower regions of the IPS do not transform to calcite, but remain amorphous. This differs from observations by Hequembourg (2002). Hequembourg (2002) suggested that the initial mineral phase was ACC that transformed to calcite along a front that followed the original deposition and was controlled by the matrix within the IPS. In this study, the mineral did not transform along a predictable front. The upper region of the IPS transformed to a crystalline mineral over time, but the middle and lower regions did not. Previous research also suggested that mineralization was complete in the cuticle by 7-8 days postecdysis (Travis, 1957; Cameron, 1985). In this study, it was shown that the mineral was deposited until 16 days postecdysis and then transformed between 16 and 32 days, this is after the start of intermolt (occurred in crabs for this study by 13 days postecdysis). This suggests that calcium and carbonate ions are still entering the cuticular layers after the beginning of intermolt. This can be explained if the ions are migrating into the cuticle by passive diffusion

from the pore canals. Specifically, the ions in the cuticle become mineral with time and this causes a decrease in the concentration gradient which allows the transfer of ions from the pore canals (high concentration gradient) to the cuticular regions (lower concentration gradient) after the start of intermolt.

This study, as well as Dillaman et al. (2005), suggests that *Callinectes sapidus* uses ACC for its isotropic properties and as a precursor phase to a more stable, crystalline mineral phase. The crab initially mineralizes the cuticle with ACC to stiffen the exoskeleton quickly after ecdysis with minimal calcification. Blue crabs use ACC to form honeycomb-shaped IPS that create a corrugated exocuticle and provide strength for the early postecdysial cuticle. Isotropic properties of amorphous mineral allows structures, like honeycomb-shaped IPS, to form that may not have been possible through direct precipitation of the crystalline phase (Mann, 2001). The amorphous mineral in the crab cuticle subsequently transforms with time and energy to a crystalline mineral for long-term strength and protection. Amorphous mineral in combination with a crystalline phase may be used by *C. sapidus* to create an exoskeleton with mechanical properties superior to a cuticle that exclusively contains one type or the other. In future studies, this understanding of the mineralization pattern and mineral phases in postecdysial and intermolt cuticle should aid in identifying, localizing, and determining the deposition of cuticular proteins that regulate calcification and ultimately, provide a better understanding of biomineralization. This is important because multiple phases of mineral have now been identified in the cuticle suggesting that there may be multiple regulatory proteins controlling the mineralization process.

LITERATURE CITED

Addadi L, Raz S, Weiner S. 2003. Taking advantage of disorder: amorphous calcium carbonate and its role in biomineralization. Adv Mater 12:959-970.

Addadi L, Weiner S, Joester D, Nudelman F. 2006. Mollusk shell formation: a source of new concepts for understanding biomineralization processes. J Chem Eur 12:980-987.

Aizenberg J, Lambert G, Addadi L, and Weiner, S. 1996. Stabilization of amorphous calcium carbonate by specialized macromolecules in biological and synthetic precipitates. Adv Mater 8:222-226.

Aizenberg J, Lambert G, Weiner S, Addadi L. 2002. Factors involved in the formation of amorphous and crystalline calcium carbonate: a study of an ascidian skeleton. J Am Chem Soc 124:32-39.

Becker A, Bismayer U, Epple M, Fabritius H, Hasse B, Shi J, Ziegler A. 2003. Structural characterization of the X-ray amorphous calcium carbonate (ACC) in the sternal deposits of the crustacean *Porcellio scaber*. J Chem Soc Dalton Trans 2003:551-555.

Becker A, Ziegler A, Matthias E. 2005. The mineral phase in cuticles of crustacea consists of magnesium calcite, amorphous calcium carbonate, and amorphous calcium carbonate. J Chem Soc Dalton Trans 2005:1814-1820.

Beniash E, Aizenberg J, Addadi L, Weiner S. 1997. Amorphous calcium carbonate transforms into calcite during sea urchin larval spicule growth. Proc R Soc Lond B 264:461-465.

Bray DF, Bagu J, Koegler P. 1993. Comparison of hexamethyldisilazane (HMDS), Peldri II, and critical-point drying methods for scanning electron microscopy of biological specimens. Micros Res Tech 26:489-495.

Bouligand Y. 1972. Twisted fibrous arrangements in biological materials and cholesteric mesophases. Tissue Cell 4:189-217.

Cameron JN. 1985. Post-moult calcification in the blue crab. National Symposium on the soft-shelled blue crab fishery. 13:31-35.

Chang E. 1995. Physiological and biochemical changes during the molt cycle in decapod crustaceans: an overview. J Exp Mar Bio Eco 193:1-14.

Clarkson JR, Price TJ, Adams CJ. 1992. Role of metastable phases in the spontaneous precipitation of calcium carbonate. J Chem Soc Faraday Trans 88:243-249.

Coblentz FE, Shafer TH, Roer RD. 1998. Cuticular proteins from the blue crab alter in vitro calcium carbonate mineralization. Comp Biochem Physiol 121B:349-360.

Compère Ph. 1995. Fine structure and morphogenesis of the sclerite epicuticle in the Atlantic shore crab, *Carcinus maenas*. Tissue Cell 27:525-538.

Compère Ph, Goffinet G. 1987. Elaboration and ultrastructural changes in the pore canal system of the mineralized cuticle of *Carcinus maenas* during the moulting cycle. Tissue Cell 19:859-875.

Compère Ph, Morgan JA, Goffinet G. 1993. Ultrastructural location of calcium and magnesium in the shore crab, as determined by K-pyroantimonate method and X-ray micoranalysis. Cell Tissue Res 274:567-577.

Dalingwater JE, Mutvei H. 1990. Arthropod exoskeletons. In: Carter JG, editor. Skeletal biomineralization: patterns, processes and evolutionary trends. Vol 1. New York: Van Nostrand Reinhold. p 1-9.

Dillaman RM, Hequembourg S, Gay DM. 2005. Early pattern of calcification in the dorsal carapace of the blue crab, *Callinectes sapidus*. J Morphol 263:356-374.

Drach P. 1939. Mue et cycle d'intermue chez les crustacés décapodes. Ann Inst Oceanogr, Monoco 19:103-391.

Fabritius H, Ziegler A. 2003. Analysis of $CaCO_3$ deposit formation and degradation during the molt cycle of the terrestrial isopod *Porcellio scaber* (Crustacea, Isopoda). J Struct Biol 142:281-291.

Giraud-Guille M. 1984. Calcification initiation sites in the crab cuticle: the interprismatic septa, an ultrastructural cytochemical study. Cell Tissue Res 236:413-420.

Green JP, Neff MR. 1972. A survey of the fine structure of the integument of the fiddler crab. Tissue Cell 4:137-171.

Greenaway P. 1983. Uptake of calcium at the postmoult stage by the marine crabs *Callinectes sapidus* and *Carcinus maenas*. Comp Biochem Physiol 75A:181-184.

Greenaway P. 1985. Calcium balance and moulting in the crustacean. Biol Rev 60:425-54.

Hadley NF. 1986. The Arthropod Cuticle. Scient Am 254:104-112.

Hegdahl T, Gustavsen F, Silness J. 1977a. The structure and mineralization of the carapace of the crab (*Cancer pagurus* L.): the exocuticle. Zool scrip 6:101-105.

Hegdahl T, Gustavsen F, Silness J. 1977b. The structure and mineralization of the carapace of the crab (*Cancer pagurus* L.): the epicuticle. Zool Scrip 6:215-220.

Hegdahl T, Silness J, Gustavsen F. 1977c. The structure and mineralization of the carapace of the crab (*Cancer pagurus* L.): the endocuticle. Zool Scrip 6:89-99.

Hequembourg S. 2002. Early patterns of calcification and protein deposition in the carapace of the blue crab. Master's Thesis, University of North Carolina at Wilmington.

Hill J, Fowler DL, Van Den Avyle MJ. 1989. Species profiles: life histories and environmental requirements of coastal fishes and invertebrates (mid-Atlantic)-Blue crab. US Fish Wildl Serv Biol Rep 82(11.100). U.S. Army Corps of Engineers, TR EL-82-4. p 1-13.

Knoll A. 2003. Biomineralization and evolutionary history. Rev Mineral Geochem 54:329-356.

Kramer K, Hopkins T, Schaefer J. 1995. Applications of solids NMR to the analysis of insect sclerotized structures. Insect Biochem Molec Biol 25:1067-1080.

Levi-Kalisman Y, Raz S, Weiner S, Addadi L, Sagi I. 2000. X-ray absorption spectroscopy studies on the structure of a biogenic "amorphous" calcium carbonate phase. J Chem Soc Dalton Trans 2000:3977-3982.

Loste E, Wilson R, Seshadri R, Meldrum F. 2003. The role of magnesium in stabilizing amorphous calcium carbonate and controlling calcite morphologies. J Cryst Morph 254:206-218.

Lowenstam H, Weiner S. 1989. On biomineralization. New York: Oxford University Press. p 25-50.

Mann, S. 2001. Biomineralization: principles and concepts in bioinorganic materials chemistry. Oxford: Oxford University Press. p 58-63.

Marlowe RL, Dillaman RM, Roer RD. 1994. Lectin binding by the crustacean cuticle: the cuticle of *Callinectes sapidus* throughout the molt cycle, and the intermolt cuticle of *Procambarus clarkii* and *Ocypode quadrata*. J Crust Biol 14:231-246.

Modla S. 2006. The effects of fixation on the morphology of the late premolt and early postmolt cuticle of the blue crab, *Callinectes sapidus*. Master's Thesis, University of North Carolina at Wilmington.

Nancollas GH. 1982. Biological mineralization and demineralization. Life Sci Res Report, Springer-Verlag, New York. p 79-100.

Passano LM. 1960. Molting and its control. In: Waterman TH, editor. The physiology of Crustacea, vol. I. Metabolism and growth. New York: Academic Press. p 473-536.

Prenant M. 1927. Les formes minéralogiques du calcaire chez les êtres vivants, et le probléme de leur déterminisme. Bio Rev 2:365-394.

Presnell JK, Schreibman MP. 1997. Humanson's animal tissue techniques. Baltimore, MD: The John Hopkins University Press. p 103.

Priester C, Dillaman RM, Gay DM. 2005. Ultrastructure, histochemistry, and mineralization patterns in the ecdysial suture of the blue crab, *Callinectes sapidus*. Microsc Microanal 11:479-499.

Raabe D, Sachs C, Romano P. 2005. The crustacean exoskeleton as an example of a structurally and mechanically graded biological nanocomposite material. Acta Mater 53:4281-4292.

Raz S, Hamilton P, Wilt F, Weiner S, Addadi L. 2003. The transient phase of amorphous calcium carbonate in sea urchin larval spicules: the involvement of proteins and magnesium ions in its formation and stabilization. Adv Funct Mater 13:480-486.

Raz S, Testieniere O, Hecker A, Weiner S, and Luguet G. 2002. Stable amorphous calcium carbonate is the main component of the calcium storage structures of the crustacean *Orchestia cavimana*. Biol Bull 203:269-274

Raz S, Weiner S, Addadi L. 2000. Formation of high-magnesian calcites via an amorphous precursor phase: possible biological implications. Adv Mater 2000:38-42.

Roer RD. 1980. Mechanisms of resorption and deposition of calcium in the carapace of the crab, *Carcinus maenas*. J Exp Biol 88:205-218.

Roer RD, Dillaman RM. 1993. Molt-related change in the integumental structure and function. In: Horst MN, Freeman JA, editors. The crustacean integument; morphology and biochemistry. Boca Raton, Florida: CRC Press. p 2-37.

Roer RD, Dillaman RM. 1984. The structure and calcification of the crustacean cuticle. Am Zool 24:893-909.

Shafer TH, Roer RD, Midgette-Luther C, Brookins TA. 1995. Postecdysial changes in the protein and glycoprotein composition of the cuticle of the blue crab, *Callinectes sapidus*: Synchronous changes in glycoproteins and mineral nucleation. J Exp Zool 271:171-82.

Simkiss K. 1975. Bone and biomineralization. London: Edward Arnold. p 1-60.

Simkiss K. 1994. Amorphous minerals in biology. Bullentin de l'Institut oceanographic Monaco, special 14:49-54.

Soejoko DS, Tjia MO. 2003. Infrared spectroscopy and X ray diffraction study on the morphological variations of carbonate and phosphate compounds in giant prawn (*Macrobrachium rosenbergii*) skeletons during its moulting period. J Mater Sci 38:2087-2093.

Spurr AR. 1969. A low viscosity epoxy resin embedding medium for electron microscopy. J Ultrastruct Res 26:31-43.

Sugawara A, Nishimura T, Yamamoto Y, Inoue H, Nagasawa H, Takashi K. 2006. Self-organization of oriented calcium carbonate/polymer composites: effects of the matrix peptide isolated from the exoskeleton of the crayfish. Angew Chem Int Ed 45:1-5.

Taylor JRA, Kier WM. 2003. Switching skeletons: hydrostatic support in molting crabs. Science 301:209-210.

Taylor MG, Simkiss K, Greaves GN, Okazaki M, Mann S. 1993. An x-ray absorption spectroscopy study of the structure and transformation of amorphous calcium carbonate from plant cystoliths. Proc R Soc Lond B 252:75-80.

Travis DF. 1955. The molting cycle of the spiny lobster *Panulirus argus* Latreille. II. Pre-ecdysial histological and histochemical changes in the hepatopancreas and integumental tissues. Biol Bull 108:88-112.

Travis DF. 1957. The molting cycle of the spiny lobster, *Panulirus argus* Latreille. IV. Post-ecdysial histological and histochemistry changes in the hepatopancreas and integumental tissues. Biol Bull 113:451-479.

Travis DF. 1963. Structural features of mineralization from tissue to macromolecular levels of organization in decapod crustacea. Ann NY Acad Sci 109:177-245.

Travis DF. 1965. The deposition of the skeletal structures in the crustacean. 5. The histomorphological and histochemical changes associated with the development and calcification of the branchial exoskeleton in the crayfish, *Orconectes virilis* Hagan. Acta Histochem 20:193-222.

Travis DF, Friberg U. 1963. The deposition of the skeletal structures in the Crustacea VI. Microradiographic studies of the exoskeleton of the crayfish, *Orconectes virilis* Hagen. J Ultrastruct Res 9:285-301.

Tweedie E, Coblentz F, Shafer T. 2004. Purification of a soluble glycoprotein from the uncalcified ecdysial cuticle of the blue crab (*Callinectes sapidus*) and its possible role in initial mineralization. J Exp Biol 207:2589-2598.

Vigh DA, Dendinger JE. 1982. Temporal relationships of postmolt deposition of calcium, magnesium, chitin and protein in the cuticle of the Atlantic blue crab, *Callinectes sapidus* rathbun. Comp Biochem Physiol Vol 72A 2:365-369.

Vinogradov AP. 1953. The elementary chemical composition of marine organisms. New Haven, CT: Sears Foundation for Marine Science Research.

Watson R, Lee K, Roer RD. 1998. Molt-inhibiting hormone mRNA levels and ecdysteroid titer during a molt cycle of the blue crab, *Callinectes sapidus*. Biochem Biophys Res Comm 249:624-627.

Weiner S, Dove P. 2003. An overview of biomineralization process and the problem of the vital effect. Rev Mineral Geochem 54:1-29.

Welinder BS. 1974. The crustacean cuticle. I. Studies on the composition of the cuticle. Comp Biochem Physiol 47A:779-87.

Welinder BS. 1975. The crustacean cuticle. III. Composition of the individual layers in *Cancer pagurus* cuticle. Biochem Physiol 52A:659-663.

Wheeler AP, George JW, Evans CA. 1981. Control of calcium carbonate crystal nucleation and crystal growth by soluble matrix of oyster shell. Science 212:1397-1398.

Wheeler AP, Rusenko KW, Swift DM, Sikes CS. 1988. Regulation of the in vitro and in vivo $CaCO_3$ crystallization by fractions of oyster shell organic matrix. Mar Biol 98:71-80.

Ziegler A. 1994. Ultrastructure and electron spectroscopic diffraction analysis of the sternal calcium deposits of *Porcellio scaber* (Isopoda, Crustacea). J Struct Biol 112:110-116.

BIOGRAPHICAL SKETCH

Samantha Jane Johnson is the daughter of Jane and David Puckett and the late Harold Dean Johnson. Samantha was born on January 8, 1978, in North Wilkesboro, North Carolina. She later moved to Gastonia, North Carolina and graduated from Ashbrook High School in 1996. In 2000, Samantha completed a Bachelor of Science degree in Marine Biology from the University of North Carolina at Wilmington. She graduated magna cum laude and received the college leadership award. In 2001, Miss Johnson accepted a Natural Science Curator I - Aquarist position at the North Carolina Aquarium at Fort Fisher. While working at the aquarium, Samantha completed her Masters of Science degree in Biology in 2006 from UNCW. She is also a member of Sigma Xi and the Master's Swim Team.